# DIGITAL DATA DETECTION

# AND SYNCHRONIZATION

by

T. L. Noack and J. F. Morris

FINAL REPORT

NGR 26-003-044



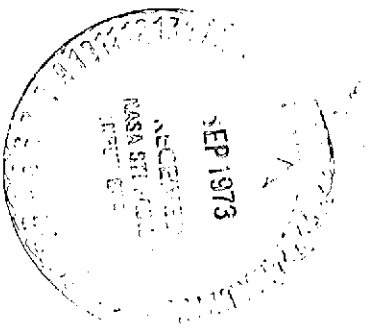

TABLE OF CONTENTS

TABLE OF CONTENTS (Cont.)

# DIGITAL DATA DETECTION AND SYNCHRONIZATION

## I. INTRODUCTION

### A. Telemetry Communication Links

The basic function of a communication link, such as that illustrated in functional block form in Figure 1, is to provide the distant destination or user with the information content of a data source in a form, and subject to a fidelity criterion, that satisfies the user. In telemetry the information originates in a variety of physical forms, such as mechanical movement, a temperature change, the occurrence of an event, a stored television image, etc. The data source usually originates the message in a nonelectrical form so that a strain gauge or temperature sensor or other form of transducer is required to produce an electrical waveform whose instantaneous values are a calibrated representation of the original source. This electrical waveform is known as an analog baseband waveform.

In a typical digital space communication link the information to be transmitted is obtained from several continuous time varying data sources. The analog data waveforms are sampled periodically and each sample is converted into a sequence of binary bits called a binary data word [1, Chapter 1]. After a predetermined number of data words has been encoded, a data word or string of words with a known code is inserted into the data stream. The known code is called a word sync or frame sync (synchronization,

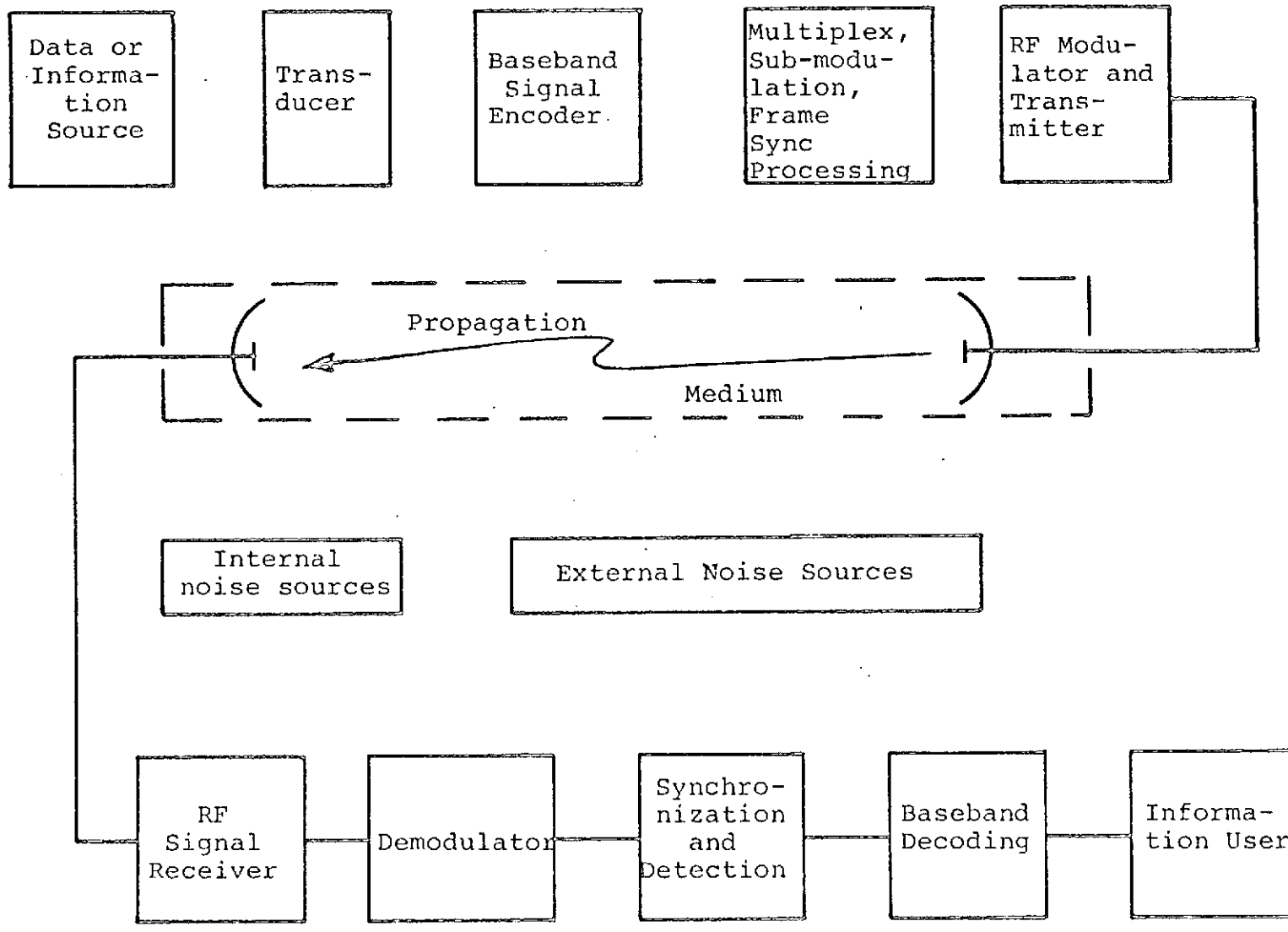


Figure 1. Functional Block Diagram of a Telemetry Communication Link

synchronizing) pattern, and is inserted so that the incoming sequence of binary waveforms can be divided into the proper words when the data is processed at the receiver. Each block of data plus the known code is referred to as a data frame. The stream of binary bits that results from this process is called the analog baseband binary data.

The baseband binary data is used to modulate a radio frequency carrier and is transmitted to a receiver through a channel which may perturb the signal through the addition of noise, fading, multipath effects of intersymbol interference due to dispersion. At the receiver the incoming radio frequency signal is demodulated or converted back to the baseband sequence. The received baseband sequence, corrupted by amplitude and phase perturbations due to the transmission channel, is what the data detector must use to construct an estimate of the original source output.

## B. Telemetry Receiver Performance

Two alternative methods are available for recording the received signals: recording either the receiver intermediate frequency (IF) section output or the detector output. The latter is the most common method, for reasons of economy and convenience. Some information is irretrievably lost by this method, but in most cases this is not a serious problem.

In occasional special cases, such as the false-lock

problem, when the receiver is locked on a strong spectral component in a sideband, rather than the carrier frequency, it could be beneficial to have both of the above signals recorded. Some insight into the false-lock problem and other receiver anomalies which produce unusual analog data output waveforms has been provided by the baseband receiver simulation (BBRS) computer program dealt with at length in an earlier report [2].

Two receiver effects are of primary importance in synchronization studies: IF filtering and carrier tracking effects. IF filtering results inevitably in some information loss, but it is necessary in order to remove adjacent channel interference, and it has been done on the existing-data. Carrier tracking is done with the phase-locked loop in the receiver IF and converter stages. It produces a low-frequency additive noise on the detector output, and it also produces acquisition, loss-of lock, and cycle slipping effects. The factors affecting carrier tracking performance are additive noise, carrier phase shifts due to doppler shift, antenna tracking effects, small amounts of multipath propagation, and loop filter characteristics. Approximate analyses have been performed by other investigators for acquisition of an offset frequency signal, a situation typical of satellite acquisition. Stiffler [1, p. 140] quotes

$$T_{\Delta f} \approx \frac{\pi^2}{4\zeta} \frac{1 + 4\zeta^2}{4\zeta} \frac{(\Delta f)^2}{B_L^3} \quad \text{secs.}$$

as the approximate lock-up time with a frequency offset and a second order loop. For the commonly used $\zeta^2 = \frac{1}{2}$ this gives

$$\frac{27\pi^2}{64B_L^3}(\Delta f)^2$$

If this gives an unacceptably long lock-up time, either a larger loop bandwidth may be used or the starting frequency may be dithered until lock-up occurs. Dithering is effective if [1, p. 142]

$$\Delta F > \frac{4}{\pi}\frac{4\zeta^2}{1+4\zeta^2} B_L .$$

Typical initial doppler shifts are less than 6Khz., and loop bandwidths are noticeably smaller than this value. Bit sync acquisition is not possible until carrier sync is acquired, and this establishes an estimate of the minimum signal-to-noise ratio in which bit synchronizer performance is of interest. Typically the carrier tracking loop will continue to track satisfactorily at baseband signal to noise ratios below the bit synchronizer performance threshold.

For split-phase data, low frequency noise added to the analog output does not significantly affect synchronization, since the data itself contains no low-frequency components. Interest in carrier tracking performance is therefore restricted to acquisition, loss-of-lock, and

cycle slipping problems. Loss-of-lock occurs when the RMS phase error becomes excessive. Its threshold is higher than the cycle slipping threshold, and it is followed by a reacquisition phase.

Cycle slipping occurs at a rate determined by the bandwidth and the signal-to-noise ratio of the loop. The rate is exponentially small at high signal-to-noise ratios. The effect of a cycle slip is shown in the following two figures.

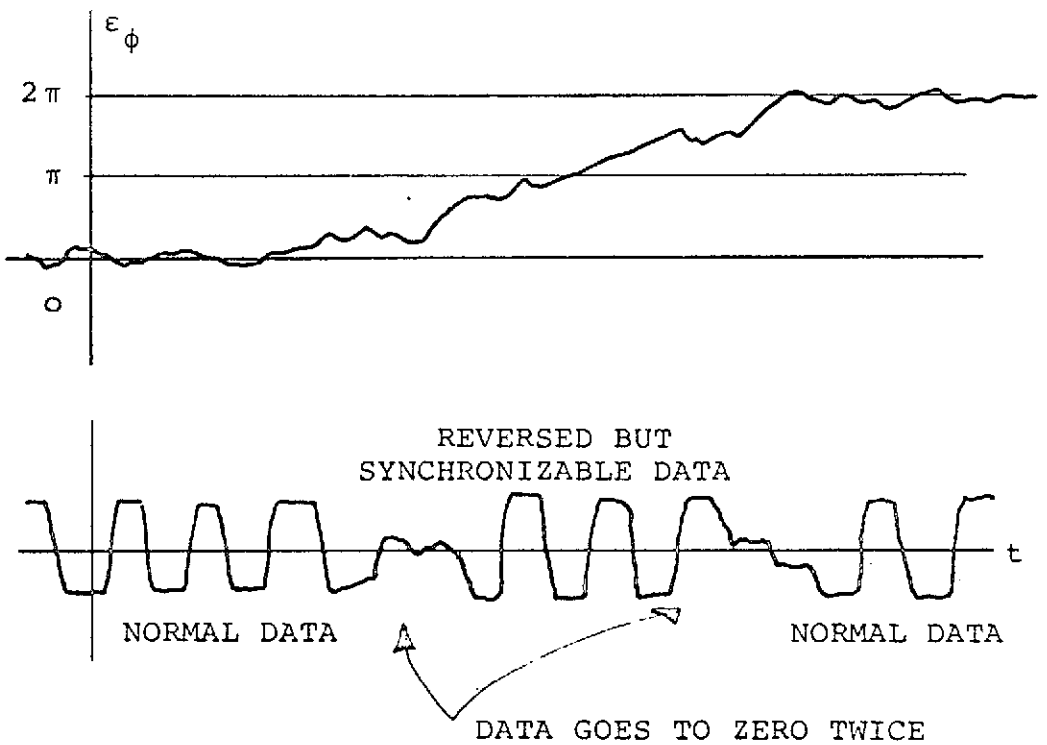


Fig. 2. Effect of Cycle Slipping on Phase Detector Outputs

The effects can be described as follows:

1. Analog signal amplitude drops to zero.

2. Analog signal output reverses, each bit is in error but signal is synchronizable.
3. Analog signal output drops to zero.
4. Conditions return to normal. In general, loss of lock in the synchronizer will not occur during this sequence if its loop equivalent bandwidth is equal to or less that of the carrier tracking loop.

## II. BIT DETECTION

### A. Classical Results

In a practical system the recorded signal is affected both by the transmitter bandlimiting filter and by receiver IF filtering. For analyses, however, the assumption of a square signal waveform plus additive white Gaussian noise allows the use of many classical results and permits the description and evaluation of the practical system in terms of the ideal model.

It is well known that if the epoch and duration of each symbol are known at the receiver the problem of detection of human signals in additive Gaussian noise has its solution in the matched filter or correlator receiver [see, for example, 3, Chapter 4]. The probability of bit error given perfect synchronization is

$$P(e) = Q(\sqrt{2E/N_0}),$$

where $E = \int_0^T s^2(t)dt$, the signal energy, $N_0$ is the one-

sided PSD and Q(X) is defined by

$$Q(X) = \frac{1}{\sqrt{2\pi}} \int_X^\infty e^{-\frac{1}{2}t^2} \, dt \ .$$

This is the minimum error probability for any given system.

With a synchronization error $\varepsilon T$ the probability of error becomes

$$P(e,\varepsilon) = \tfrac{1}{2}Q\left[\sqrt{\frac{2E}{N_o}}(1 - f_e(\varepsilon))\right] + \tfrac{1}{2}Q\left[\sqrt{\frac{2E}{N_o}}(1 - f_o(\varepsilon))\right],$$

where $(1 - f_e(\varepsilon)) = \frac{1}{E} \int_0^T s(t)[s(t - \varepsilon T) + s(t + T - \varepsilon T)]dt$

for $\varepsilon > 0$, and $(1 - f_o(\varepsilon)) = \frac{1}{E} \int_0^T s(t)[s(t - \varepsilon T) - s(t + T - \varepsilon T)]dt$ .

The value of $P(e,\varepsilon)$ given by this relationship is based on equiprobable and independent adjacent bits. The probability of error for a given synchronization error distribution $P_\phi(\varepsilon)$ is

$$P_s(e) = \int_{-\frac{1}{2}}^{\frac{1}{2}} P(e,\varepsilon)P_\phi(\varepsilon) \, d\varepsilon \ .$$

This expression can be used to evaluate the effect of synchronizer performance on error probability. A useful normalized version of timing error is given by

$$\Lambda = \frac{\text{Var } (\varepsilon)}{2E/N_o}.$$

It can be shown for square split-phase signals, that the signal power degradation is approximated by $(1 + 16\Lambda)^{-1}$ in power. The factor $\Lambda$ can be related to synchronizer loop bandwidth X bit period X synchronizer performance factor. For example, for a common type of early-late gate $\Lambda$ is given by $\frac{6B_R}{\Delta B_L}$ where $B_R$ is the bit rate, $B_L$ is the tracking loop bandwidth and $\Delta$ is the window width in fractions of a bit. This approximation is good for high signal-to-noise ratio and weaker for low SNR.

B. Decision-Directed Detector for Overlapping Symbols

When a binary data stream is received over a practical communication system errors in bit detection may be caused by intersymbol interference. This channel-induced distortion is due to the fact that, because the system is narrow band, each symbol may overlap with symbols in the preceding and following intervals. The amount of distortion depends on the symbol sequence, symbol duration, and the channel bandwidth.

Various methods for correcting the bit decision in the presence of intersymbol interference have been considered. Aaron and Tufts [4] suggested a method based on the use of tapped delay lines to match the channel. They

account for the intersymbol interference by finding the optimum tap positions and gain coefficients for the given channel. Helstrom [5] suggested a different method. He suggested a system that uses the last three bits received for making a decision. He considers all eight possible bit configurations by looking at three at a time, and then he uses the known channel characteristics to outline the design of seven different filters. A decision system is then used to choose the filter with the largest output as the received PCM signal. Both Aaron's and Helstrom's methods have a serious disadvantage in the fact that the design procedure of these matched filters is very complicated for any specified channel. Three suggested systems for making a decision in the presence of intersymbol interference and Gaussian noise are presented by Thumim [6] which have the advantage that the parameters can be easily changed to adjust the changes in the channel.

As part of the research under this grant, Wang [7] has developed the model for a new decision-directed detector for overlapping symbols. Analytical results and computer simulation results are presented as curves of probability of error versus signal-to-noise ratio.

Basically, two steps are involved in his approach. First, the symbol most likely received is determined as a primary decision. Then, this decision is used to direct the detection process to obtain a better estimate of the

symbol which will yield less probability of error. For overlapping signals, the DD technique can be roughly summarized in Figure 4.1. The post-bit detector consists of an ordinary matched filter and a sampler. The input signals are processed serially, one after the other, and the output is the primary detected value, $\hat{a}_p$. The function of the block "SHAPE" is to maintain a constant level until the next sampling instant. The output is then used to subtract the overlapping tail resulting from the next bit. With the subtraction of the overlapping head from the preceding bit, a present-bit detector is followed to find the final decision. The overlapping head and tail are illustrated in Figure 4.2.

Since both detectors in Figure 4.1 perform the same function, they can be placed in the front as a detector. The modified structure for the DD detector is shown in Figure 4.3. Here the decision devices are replaced by two hard limiters. The constants $K_2$ and $K_3$ will be introduced in the following section.

1. Mathematical Derivation

The binary communication system under consideration consists of two symbols, $S_p(t)$ and $-S_p(t)$, defined in Figure 4.2. The received signal is

$$y(t) = \sum_{k=1}^{m} a_k \, S_p(t - k) + n(t) \qquad (4.1)$$

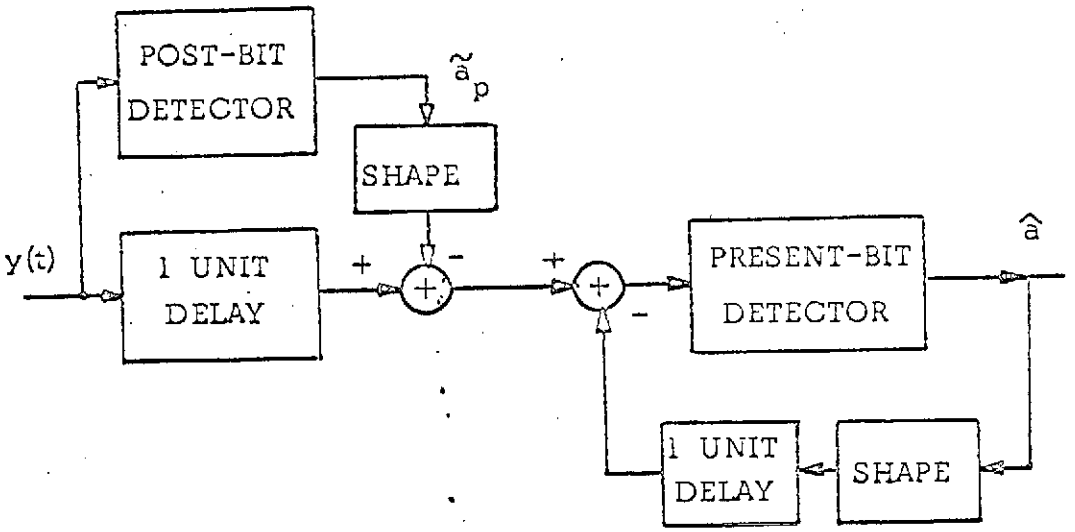


Fig.4.1 Decision-directed detector for overlapping signals

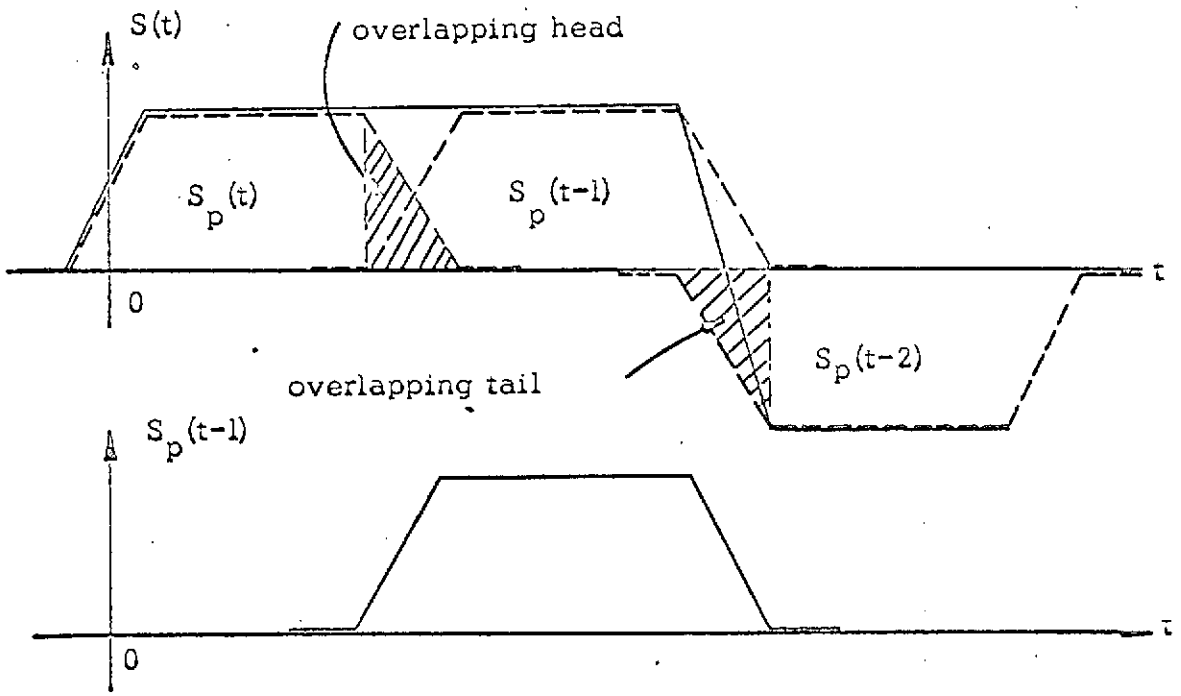


Fig.4.2 Received signal and the overlapping symbol

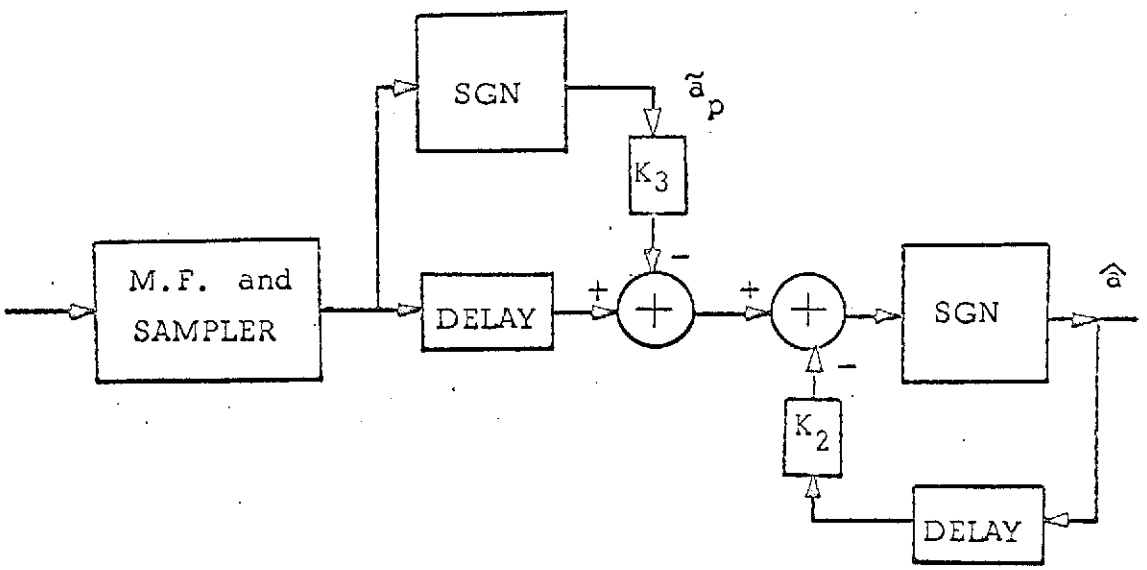


Fig. 4.3 Modified decision-directed detector

The matched filter has an impulse response

$$h(t) = S_p(1 - t)$$

Thus the output of the matched filter is

$$z(t) = y(t) * h(t)$$

$$= \sum_{k=1}^{m} a_k S_p(t - k) * S_p(1 - t) + n(t) * S_p(1 - t) \tag{4.2}$$

At the sampling instant $t = i$,

$$z(i) = \sum_{k=1}^{m} a_k S_p(i - k) * S_p(1 - i) + n(i) * S_p(1 - i) \tag{4.3}$$

Due to the overlapping situation, $z(i)$ can be further written as

$$z(i) = K_2 a_{i-1} + K_1 a_i + K_3 a_{i+1} + K_4 n(t) \tag{4.4}$$

where $K_2$ and $K_3$ are the areas when dealing with overlap of the ith bit with the (i-1)th bit and with the (i+1)th bit, respectively. $K_1$ is the area when the ith bit convolves with itself. $K_4$ is the noise coefficient to be defined later. These constants are functions of $\theta$, and are required in the simulation program. The calculation of $K_1$, $K_2$, and $K_3$ proceeds as follows.

$$K_2 = \int_{k-\alpha}^{k+1+\alpha} S_p(t-k)S_p(t-k+1)\,dt$$

$$= \int_{-\alpha}^{1+\alpha} (1/2 + t/2\alpha)(1/2 - t/2\alpha)\,dt = \alpha/3. \qquad (4.5)$$

$$K_1 = \int_{-\alpha}^{1+\alpha} S_p^2(t)\,dt = \alpha/3 + (1 - 2\alpha) + \alpha/3$$

$$= 1 - 2\alpha/3, \text{ and} \qquad (4.6)$$

$$K_3 = K_2 = \alpha/3. \qquad (4.7)$$

To find $K_4$, we consider the root mean square of the correlator output when the signal is correlated with noise. That is

$$E \left[ \int_{-\alpha}^{1+\alpha} S_p(t)n(t)\,dt \right]^2$$

$$= \int_{-}^{1+\alpha}\int S_p(t_1)S_p(t_2)\; E\, n(t_1)n(t_2)\; dt_1\, dt_2$$

$$= B \int_{-\alpha}^{1+\alpha} S_p^2(t)\,dt = B(1 - 2\alpha/3) \qquad (4.8)$$

Where B is taken as the reciprocal of the input signal-to-noise ratio in the simulation program. The noise coefficient $K_4$ is then $K_4 = \sqrt{1 - 2\alpha/3}$.

## 2. Simulation Program

In general, the desired output is a graph of $P_E$ versus SNR with the overlapping parameter $\alpha$ as a parameter. In order to examine how much improvement can be achieved by the DD technique, two error probabilities are tabulated in parallel. That is, for each bit, a primary decision by non-decision-directed measurement is made. At the end of m bits, the probability of error of the primary decision is computed. Then the final decision on each bit using the DD measurement is found.

In the simulation program 500 bits are generated at random and used as input to the DD detector. The probability of error is approximated by the ratio of the total number of erroneous bits to the total number of input bits. The resultant error counts for several values of $\alpha$ are shown on succeeding pages.

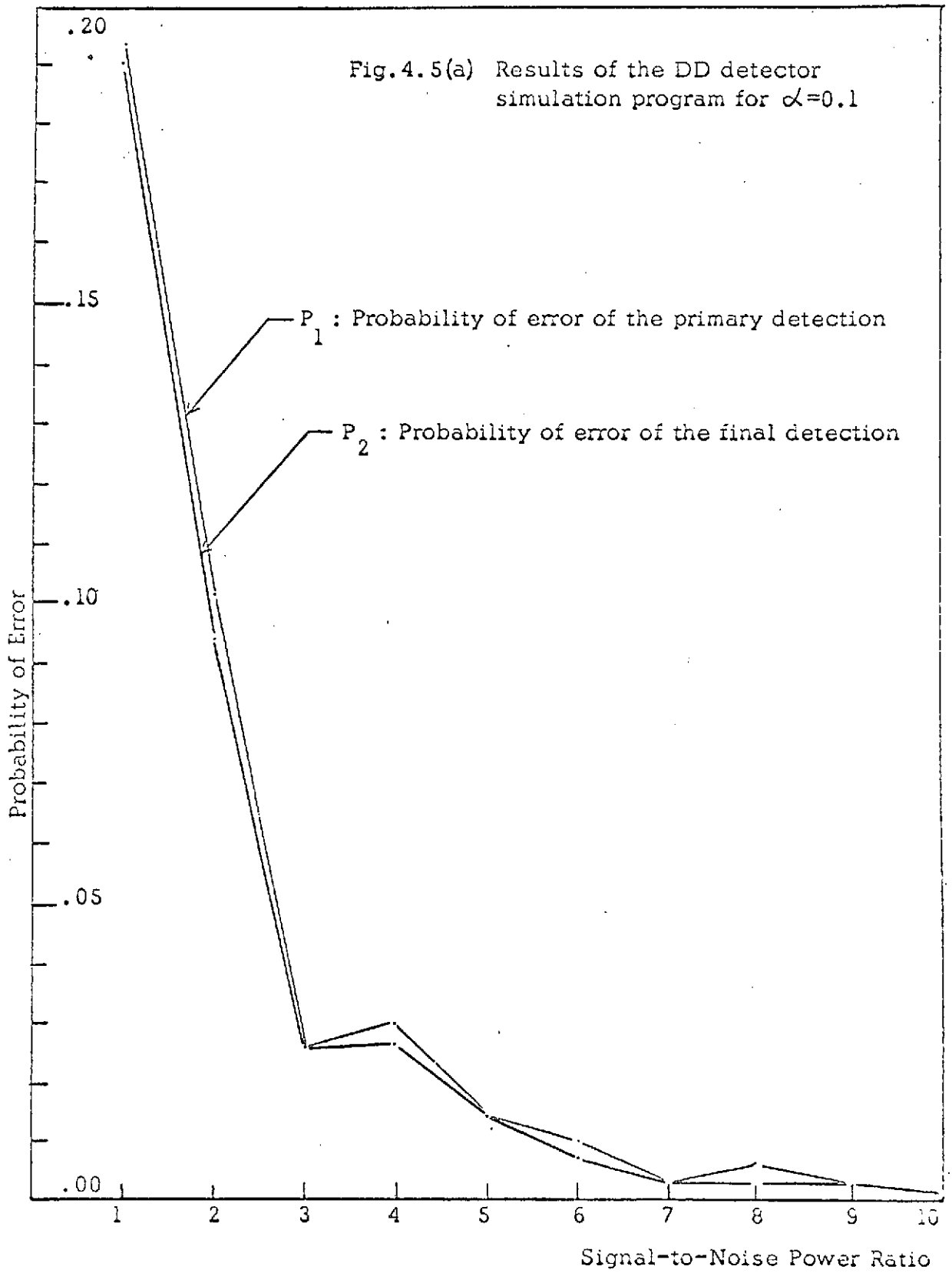


Fig. 4.5(a) Results of the DD detector simulation program for $\alpha$=0.1

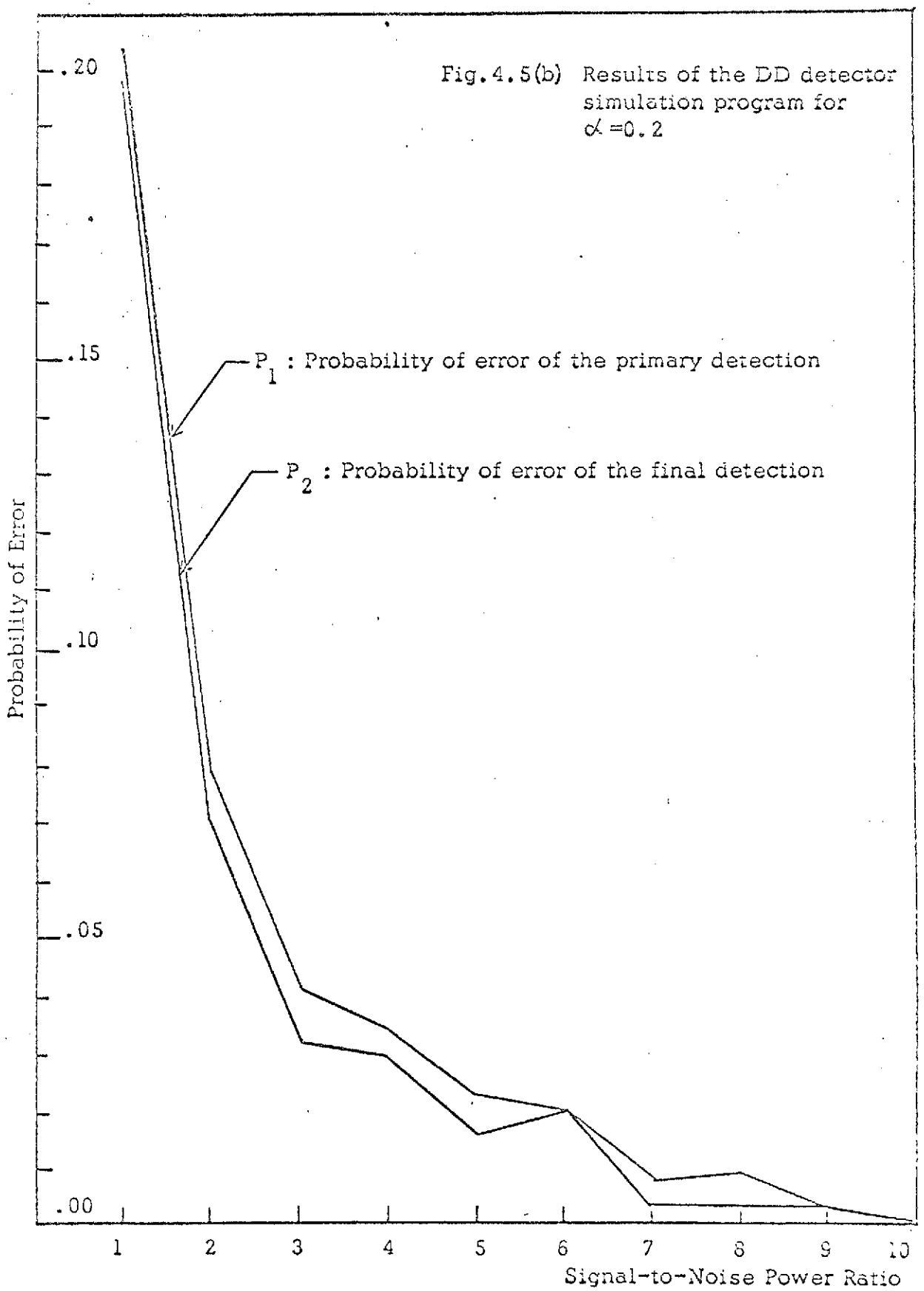


Fig. 4.5(b) Results of the DD detector simulation program for $\alpha = 0.2$

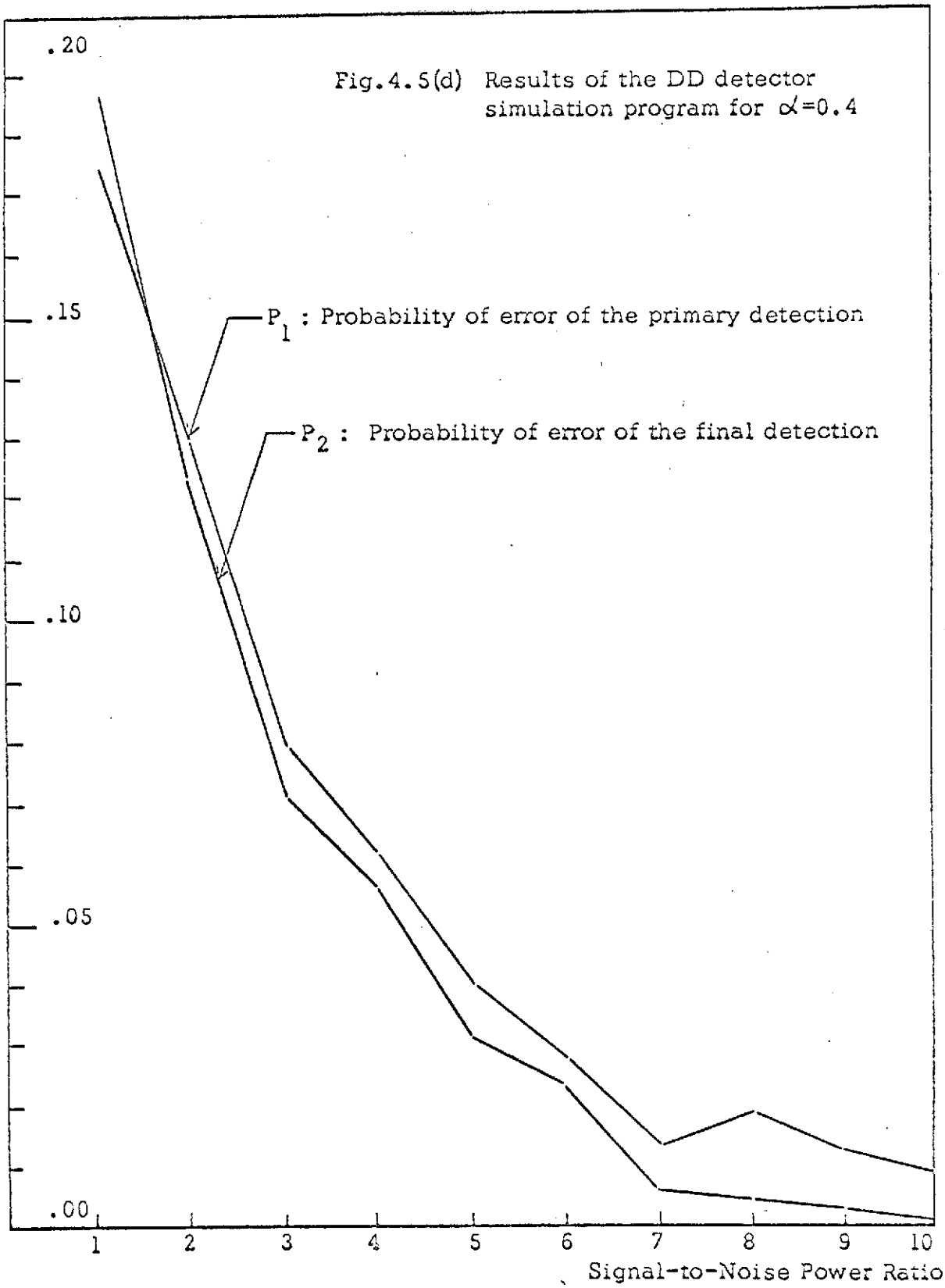


Fig.4.5(d) Results of the DD detector simulation program for $\alpha=0.4$

## 3. Analytical Results

In this section, calculation of $P_E$ for the DD detector is considered. The block diagram of a DD detector is redrawn in Figure 4.6.

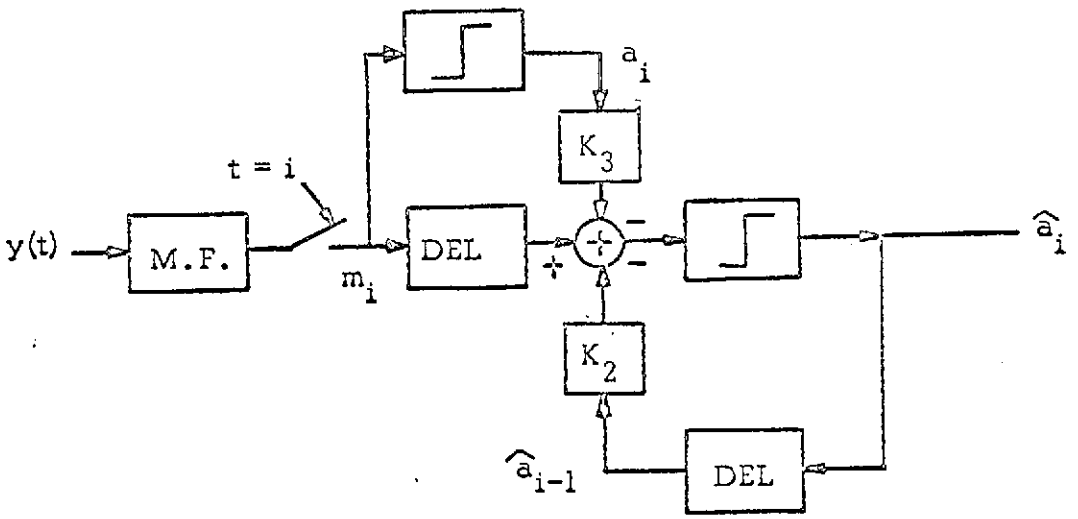


Fig. 4.6. Block diagram of the DD detector

The output of the matched filter and sampler is

$$m_i = K_2\, a_{i-1} + K_1\, a_i + K_3\, a_{i+1} + K_4\, n_i \qquad (4.9)$$

where $K_1 = 1 - (2/3)\alpha$

$K_2 = K_3 = (1/3)\alpha$, and

$K_4 = \sqrt{1 - (2/3)\alpha}$ .

Because of the overlapping situation, three symbols are involved in determining the probability of bit error

of the primary detection. Let $A = (a_{i-1}, a_i, a_{i+1})$; the eight possible combinations of the sequence are tabulated in Table 4.3. The $P_E$ of the primary detection is

$$\tilde{P} = P\{m_i < 0 \mid a_i = 1\}\ P\{a_i = 1\}$$

$$+ P\{m_i > 0 \mid a_i = -1\}\ P\{a_i = -1\} \qquad (4.10)$$

Table 4.3 Eight possible sequences and mean values for finding the primary $P_E$

| | $a_{i-1}$ | $a_i$ | $a_{i+1}$ | $E(m_i) = \mu_i$ | $var(m_i) = \sigma^2$ |
|---|---|---|---|---|---|
| $A_1$ | 1 | 1 | 1 | 1 | $\sigma = \sqrt{B(1 - (2/3)\alpha)}$ |
| $A_2$ | -1 | 1 | 1 | $1 - (2/3)\alpha$ | |
| $A_3$ | 1 | 1 | -1 | $1 - (2/3)\alpha$ | |
| $A_4$ | -1 | 1 | -1 | $1 - (4/3)\alpha$ | |
| $A_5$ | 1 | -1 | 1 | $-1 + (4/3)\alpha$ | $B = 1/SNR$ |
| $A_6$ | -1 | -1 | 1 | $-1 + (2/3)\alpha$ | |
| $A_7$ | 1 | -1 | -1 | $-1 + (2/3)\alpha$ | |
| $A_8$ | -1 | -1 | -1 | -1 | |

When we consider $a_i = 1$, there are four possible sequences, $(A_1, A_2, A_3, A_4)$, involved in finding the term $P\{m_i < 0 \mid a_i = 1\}$. Thus,

$$P\ m_i < 0 \,\Big|\, a_i = 1 \;=\; (1/4) \sum_{j=1}^{4} \int_{-\infty}^{0} (1/\sqrt{2\pi}\sigma)\ \exp - \frac{(x - \mu_j)^2}{2}\ dx,$$

where $\mu_i \triangleq E\{m_i\}$. Treating the case for $a_i = -1$ in the same manner, we have

$$\tilde{P} = (1/2)\quad (1/4) \sum_{j=1}^{4} \int_{-\infty}^{0} (1/\sqrt{2\pi}\sigma)\ \exp\ - \frac{(x - \mu_j)^2}{2}\ dx$$

$$+\ (1/4) \sum_{j=5}^{8} \int_{0}^{\infty} (1/\sqrt{2\pi}\sigma)\ \exp\ - \frac{(x - \mu_j)^2}{2}\ dx$$

$$= (1/8) \sum_{j=1}^{4} \phi(-\mu_j/\sigma) + \sum_{j=5}^{8} \phi(\mu_j/\sigma). \qquad (4.11)$$

$$\text{where } \phi(a) = \int_{-\infty}^{a} (1/\sqrt{2\pi}) \cdot \exp(-x^2/2)\ dx \qquad (4.12)$$

Substituting mean values, (4.11) can be simplified as follows.

$$\tilde{P} = (1/4)\{\phi(-1/\sigma) + 2\ \phi(-(1 - 2\alpha/3)/\sigma) + \phi(-(1 - 3\alpha/4)/\sigma)\} \qquad (4.13)$$

The probability of the final detection is found as follows. Since the final decision $\hat{a}_i$ depends on the previous final decision $\hat{a}_{i-1}$ and on the primary decision on (i+1)th bit, $\hat{a}_{i+1}$, we have

$$\hat{a}_i = m_i - K_3\ \tilde{a}_{i+1} - K_2\ \hat{a}_{i-1} \qquad (4.14)$$

where $m_i = K_2\ a_{i-1} + K_1\ a_i + K_3\ a_{i+1} + K_4\ n_i$

Hence, the probability of error is described by a recursive relation. Let us define

$$P_i \triangleq \{P\ \hat{a}_i < 0 \mid a_i, \tilde{a}_{i+1}, \hat{a}_{i-1}\}\ P\{a_i\}\ P\{\tilde{a}_{i+1}\}\ P\{\hat{a}_{i-1}\} \tag{4.15}$$

Rewriting (4.14) by substituting $m_i$ in the equation, we have

$$\hat{a}_i = K_2\ (a_{i-1} - \hat{a}_{i-1}) + K_1\ a_i + K_3\ (a_{i+1} - \tilde{a}_{i+1}) + K_4\ n_i \tag{4.16}$$

If the primary decision on the symbol $a_i$ is correct, the final output of the detector will be just a constant, $K_1$, times $a_i$. It can be seen from the simulated results that at high SNR the probability of error for the final detection decreases faster than that of the primary detection.

The probability of error for the final detection, $P_i$, is

$$\begin{aligned} P_i = {} & P\{\hat{a}_i < 0 \mid a_i=1, \tilde{a}_{i+1}=a_{i+1}, \hat{a}_{i-1}=a_{i-1}\}(1/2)(1-\tilde{P})(1-P_{i-1}) \\ & + P\{\hat{a}_i < 0 \mid a_i=1, \tilde{a}_{i+1}=a_{i+1}, \hat{a}_{i-1}\neq a_{i-1}\}(1/2)(1-\tilde{P})\ P_{i-1} \\ & + P\{\hat{a}_i < 0 \mid a_i=1, \tilde{a}_{i+1}\neq a_{i+1}, \hat{a}_{i-1}=a_{i-1}\}(1/2)\ \tilde{P}\ (1-P_{i-1}) \\ & + P\{\hat{a}_i < 0 \mid a_i=1, \tilde{a}_{i+1}\neq a_{i+1}, \hat{a}_{i-1}=a_{i-1}\}(1/2)\ \tilde{P}\ P_{i-1} \\ & + \text{four terms for } a_i = -1. \end{aligned} \tag{4.17}$$

Table 4.4 Possible sequences and mean values for finding the final $P_E$

| $a_i$ | | $E[\hat{a}_i] \triangleq \eta_i$ |
|---|---|---|
| 1 | $a_{i-1}=\hat{a}_{i-1}$, $a_{i+1}=\tilde{a}_{i+1}$ | $\eta_1 = K_1$ |
| 1 | $a_{i-1}\neq\hat{a}_{i-1}$, $a_{i+1}=\tilde{a}_{i+1}$ | $\eta_2 = 2 K_2 a_{i-1} + K_1$ |
| 1 | $a_{i-1}=\hat{a}_{i-1}$, $a_{i+1}\neq\tilde{a}_{i+1}$ | $\eta_3 = K_1 + 2 K_3 a_{i+1}$ |
| 1 | $a_{i-1}\neq\hat{a}_{i-1}$, $a_{i+1}\neq\tilde{a}_{i+1}$ | $\eta_4 = 2 K_2 a_{i-1} + K_1 + 2 K_3 a_{i+1}$ |
| -1 | $a_{i-1}=\hat{a}_{i-1}$, $a_{i+1}=\tilde{a}_{i+1}$ | $\eta_5 = -K_1$ |
| -1 | $a_{i-1}\neq\hat{a}_{i-1}$, $a_{i+1}=\tilde{a}_{i+1}$ | $\eta_6 = 2 K_2 a_{i-1} - K_1$ |
| -1 | $a_{i-1}=\hat{a}_{i-1}$, $a_{i+1}\neq\tilde{a}_{i+1}$ | $\eta_7 = -K_1 + 2 K_3 a_{i+1}$ |
| -1 | $a_{i-1}\neq\hat{a}_{i-1}$, $a_{i+1}\neq\tilde{a}_{i+1}$ | $\eta_8 = 2 K_2 a_{i-1} - K_1 + 2 K_3 a_{i+1}$ |

Setting $1 - P_{i-1} = Q$, $P_{i-1} = P$, $1 - \tilde{P} = \tilde{Q}$, we have

$$P_i = (Q\tilde{Q}/2) \int_{-\infty}^{0} N(\eta_1,\sigma)\, dx + (P\tilde{Q}/2) \int_{-\infty}^{0} N(\eta_2,\sigma)\, dx$$

$$+ (\tilde{P}Q/2) \int_{-\infty}^{0} N(\eta_3,\sigma)\, dx + (P\tilde{P}/2) \int_{-\infty}^{0} N(\eta_4,\sigma)\, dx$$

$$+ (Q\tilde{Q}/2) \int_{0}^{\infty} N(\eta_5,\sigma)\, dx + (P\tilde{Q}/2) \int_{0}^{\infty} N(\eta_6,\sigma)\, dx$$

$$+ (Q\tilde{P}/2) \int_{0}^{\infty} N(\eta_7,\sigma)\, dx + (P\tilde{Q}/2) \int_{0}^{\infty} N(\eta_8,\sigma)\, dx. \qquad (4.18)$$

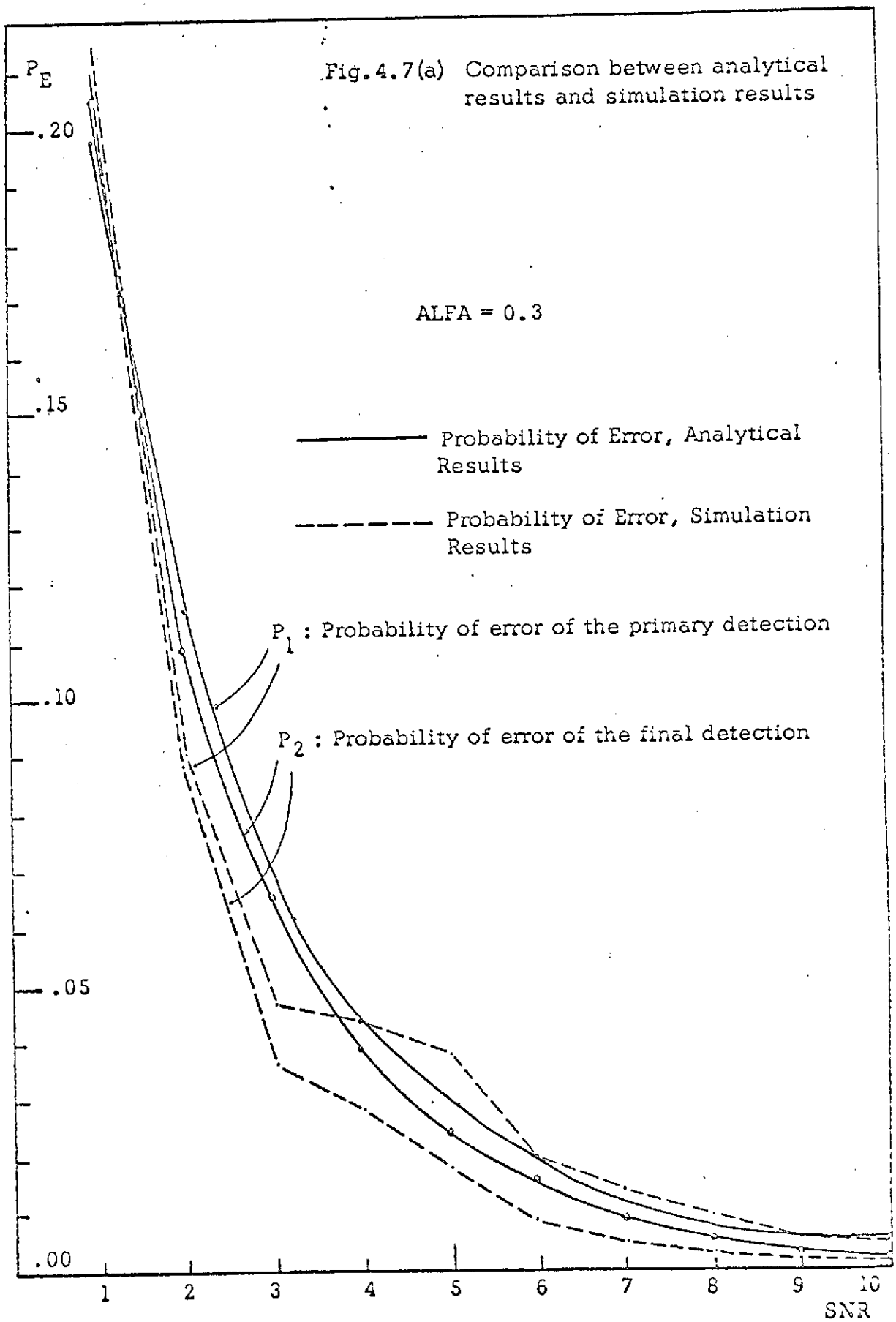


Fig. 4.7(a) Comparison between analytical results and simulation results

Fig.4.7(b) Comparison between analytical results and simulation results

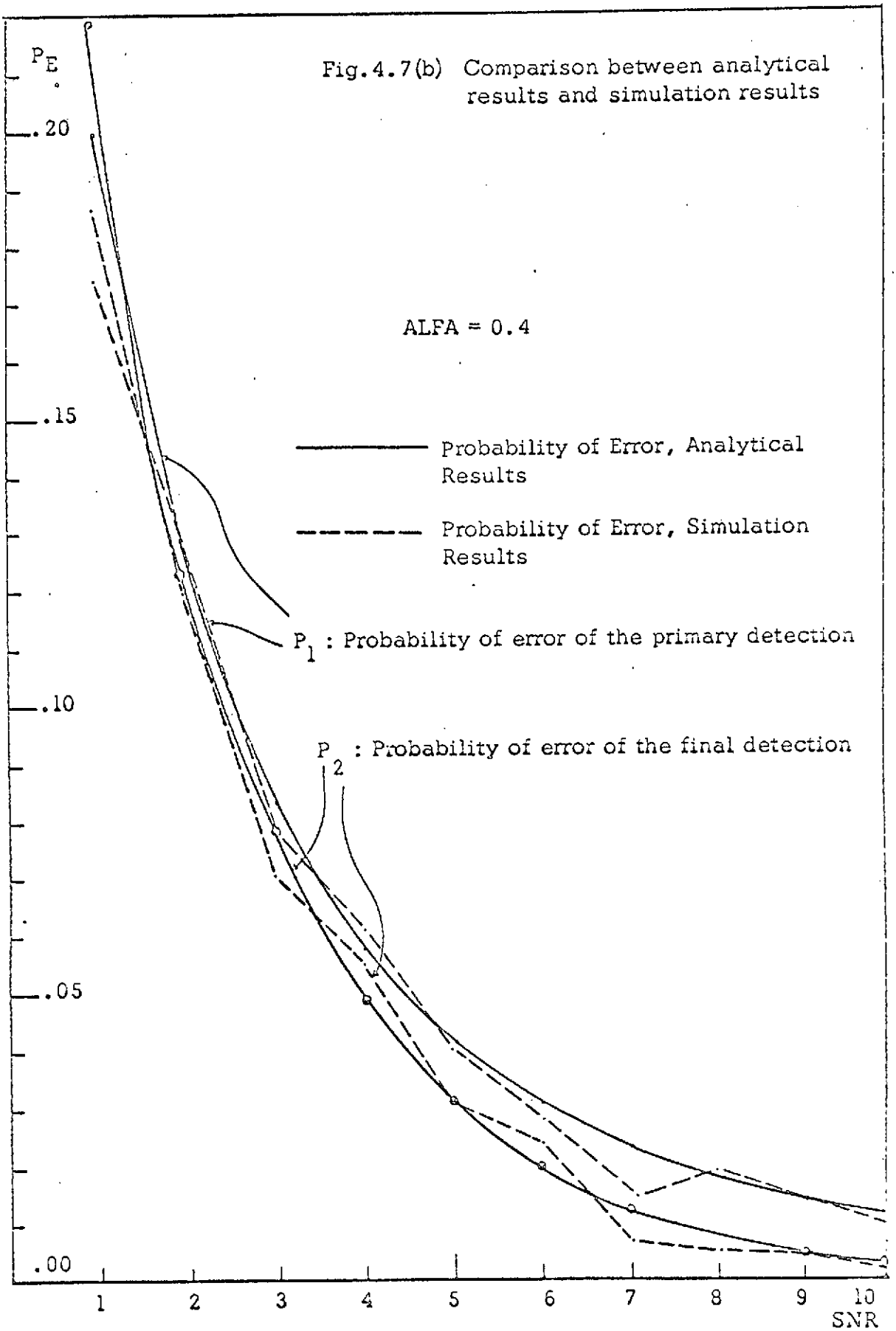

Table 4.5 Program for evaluating the primary $P_E$ and the final $P_E$

```
      REAL K1,K2,K3,P(10),Q(10)
   99 READ(1,100,END=999) SNR,ALFA
  100 FORMAT(2F5.2)
C
      K1 = 1.-2.*ALFA/3.
      K2 = ALFA/3.
      K3 = K2
      SIGMA = SQRT((1.-2.*ALFA/3.)/SNR)
      A = -1./SIGMA
      B = -K1/SIGMA
      C = -(1.-4.*ALFA/3.)/SIGMA
C  COMPUTE THE PRIMARY PROBABILITY OR ERROR
      P1 = 0.25*(PHI(A) + 2.*PHI(B) + PHI(C))
      WRITE(3,101) SNR,ALFA,P1
  101 FORMAT(/5X'SNR='F5.2,5X,'ALFA='F5.2,5X,'PRIMAY P(E) IS',
     1   F16.7)
C
      Q1 = 1.-P1
      P(1) = 0.0
      Q(1) = 1.-P(1)
      C1 = PHI(-K1/SIGMA)
      C2 = PHI(-(K1-2.*k2)/SIGMA) + PHI(-(K1+2.*K2)/SIGMA)
      C3 = PHI(-(K1-K3)/SIGMA) + PHI(-(K1+K3)/SIGMA)
      C4 = PHI(-(K1-2.*K2-2.*K3)/SIGMA) + PHI(-(K1+2.*K2+2.*K3)
     2   /SIGMA) + PHI(-(K1-2.*K2+2.*K3)/SIGMA)+PHI(-(K1+2.*K2
     3   -2.*K3)/SIGMA)
C  COMPUTE THE FINAL PROBABILITY OF ERROR
      DO 2 I=2,10
      P(I) = Q1*Q(I-1)*C1 + Q1*P(I-1)*0.5*C2 + P1*Q(I-1)*0.5*C3 +
     4    Q1*P(I-1)*0.25*C4
      Q(I) = 1.-P(I)
      WRITE(3,102) I,P(I)
  102 FORMAT(/15X,'P(',I2,')=',F16.7)
  2   CONTINUE
      GO TO 99
  999 STOP
      END
```

(continue on the next page)

(Table 4.5 continued)

```
        FUNCTION  PHI(X)
        AX = ABS(X)
        T = 1.0/(1.0+0.2316419*AX)
        D = 0.3989423*EXP(-X*X/2.0)
        P = 1.0-D*T*((((1.330274*T-1.821256)*T+1.781478)*T-
       1    0.3565638)*T+0.3193815)
        PHI = P
        IF(X) 1,2,2
  1     PGI = 1.0-P
  2     RETURN
        END
/DATA
/END
```

where the notation $N(\eta_i,\sigma)$ indicates the density function of a Gaussian distribution having a mean value $\eta_i$, and a variance $\sigma^2$. Now we can substitute the values for $\eta_i$, $i = 1, 2, \ldots, 8$, and write $P_i$ as the function of the $\phi$-function defined by (4.12). Note that $\phi(-x) = 1 - \phi(x)$. (4.18) can be further simplified by using this identity. Therefore,

$$\begin{aligned} P_i = {} & [Q\tilde{Q}]\ \phi(-K_1/\sigma) + (PQ/2)\ [\phi(-(K_1-2K_2)/\sigma) + \phi(-(K_1+2K_2)/\sigma)] \\ & + (Q\tilde{P}/2)\ [\phi(-(K_1 - K_3)/\sigma) + \phi(-(K_1 + K_3)/\sigma)] \\ & + (P\tilde{P}/2)\ [\phi(-(K_1 - 2\,K_2 - 2K_3)/\sigma) + \phi(-(K_1 + 2\,K_2 + 2\,K_3)/\sigma) \\ & \qquad + \phi(-(K_1 - 2\,K_2 + 2K_3)/\sigma) + \phi(-(K_1 + 2\,K_2 - 2\,K_3)/\sigma)] \end{aligned} \tag{4.19}$$

The analytical results of the primary $P_E$ and the final $P_E$ can be evaluated by a computer program shown in Table 4.5. The results are plotted with the simulation data found in the last section to see how closely they are related. It is seen from Figure 4.7 that when $\alpha = 0.3$ and 0.4, the analytical results and the simulation results are in good agreement.

## III. BIT SYNCHRONIZATION

### A. Synchronizers for Non-Overlapping Symbols

Wintz and Luecke [8] derived the optimum synchronizer, in the maximum likelihood sense, for binary non-overlapping symbols in Gaussian noise. The starting point is the

derivation of the relationship for $p(Y|\theta)$, where Y is the observation $y(t)$ for $t\varepsilon(o,nT)$. The maximum likelihood synchronizer is a device for computing this probability as a function of $\theta$ and then choosing the value of $\theta$ which maximizes the expression. The probability $p(Y|\theta)$ is computed by first finding $p(Y|\theta,\bar{a})$ where $\bar{a}$ is the bit sequence $a_0, a_1, a_2 \ldots a_{N-1}$. Then $p(Y|\theta,\bar{a})$ is given by

$$p(Y|\theta) = \sum_{\text{All } \bar{a}} p(Y|\theta,\bar{a})\ p(\bar{a})$$

The $p(\bar{a})$ used is the A priori probability of any given bit sequence, assuming all $2^N$ are equally likely. This gives rise to the expression

$$p(Y|\theta) \approx \prod_{0}^{N-1} \text{COSH}\left[\frac{1}{N_o}\int_0^T y(t + jT + \theta)s(t)\ dt\right]$$

$$\text{or } \ln p(Y|\theta) = C + \sum_{j=0}^{N-1} \log \text{COSH}\left[\frac{1}{N_o}\int_0^T y(t + jT + \theta)s(t)\ dt\right]$$

The synchronizer then maximizes this likelihood function. The function log cosh(x) is an interesting one: for small $|x|$ it is approximately $\frac{x^2}{2}$, while for large $|x|$ it is approximately $|x| - \ln 2$. The expression

$$\sum \log \text{COSH}\ \frac{1}{N_o}\int_0^T y(t + jT + \theta)s(t)\ dt = \psi_j$$

$$= \int_{-\theta}^{T-\theta} y(t + jT)s(t - \theta)\ dt$$

may be obtained from a correlator with an integrate-and dump.

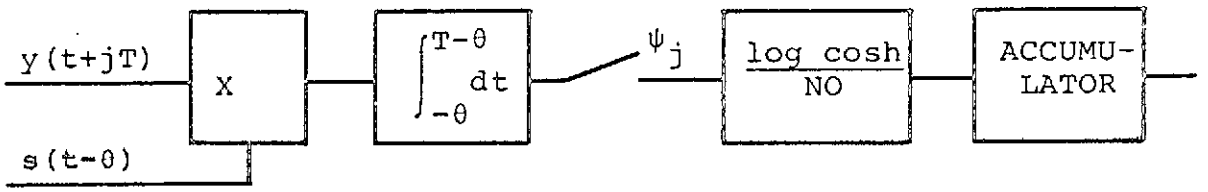


The maximum likelihood synchronizer is mechanized by a bank of these units followed by a unit which selects the $\theta_i$ which produces the maximum output.

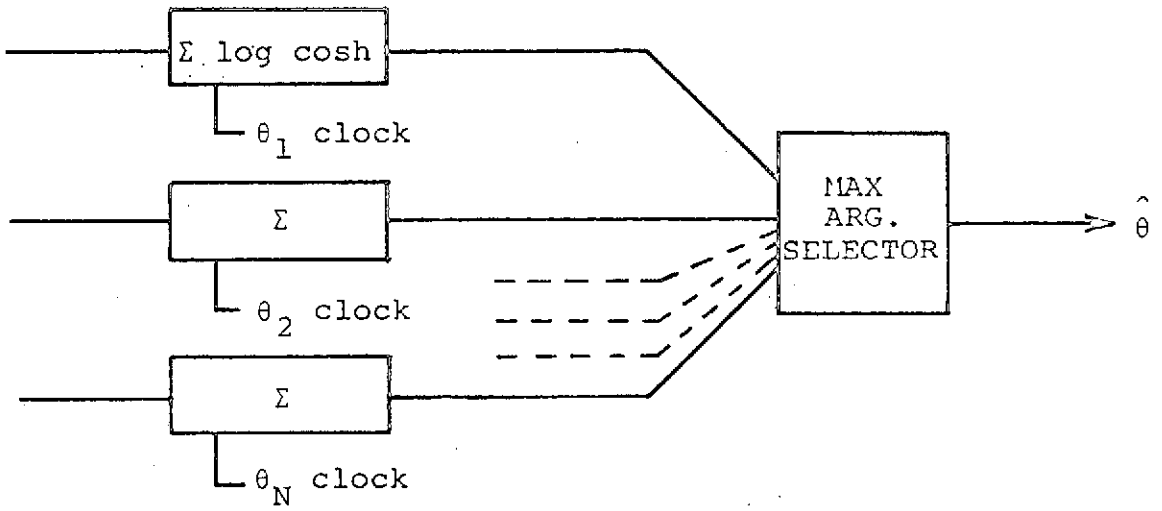


For continuous signals this synchronizer can be greatly simplified. If we write

$$L(\theta) = \sum \log \text{COSH} \frac{1}{N_o} \int_{-\theta}^{T-\theta} y(t + jT)s(t - \theta)\, dt$$

At this point it is convenient to introduce an inner product notation

$$\int_0^T y(t + jT)s(t)\,dt \triangleq \langle y_j, s\rangle$$

then $$s(t - \theta) \cong s(t) - \theta\, s'(t)$$

and $$L(\theta) = \sum \log \text{COSH}\, \frac{1}{N_o}\,[\langle y_j, s\rangle - \theta\langle y_j, s'\rangle]$$

the optimum estimate $\hat{\theta}$ is found by

$$N_o \frac{\partial L}{\partial \theta} = 0 = \sum \langle y_j, s\rangle \tanh[\frac{1}{N_o}(\langle y_j, s\rangle - \theta\langle y_j, s'\rangle)].$$

Expanding $\tanh(X + \theta\varepsilon) = \tanh X + \theta\varepsilon\ \text{sech}^2 X$,

$$0 = \sum \langle y_j, s'\rangle \tanh(\frac{1}{N_o}\langle y_j, s\rangle) - \theta \sum \frac{1}{N_o}\langle y_j, s'\rangle^2 \text{sech}^2 \frac{1}{N_o}\langle y_j, s\rangle$$

which yields

$$\theta = \frac{\sum \langle y_j, s'\rangle \tanh(\frac{1}{N_o}\langle y_j, s\rangle)}{\sum \frac{1}{N_o}\langle y_j, s'\rangle^2 \text{sech}^2 \frac{1}{N_o}\langle y_j, s\rangle}$$

The denominator converges to a constant times the number of bits, and the resulting configuration is

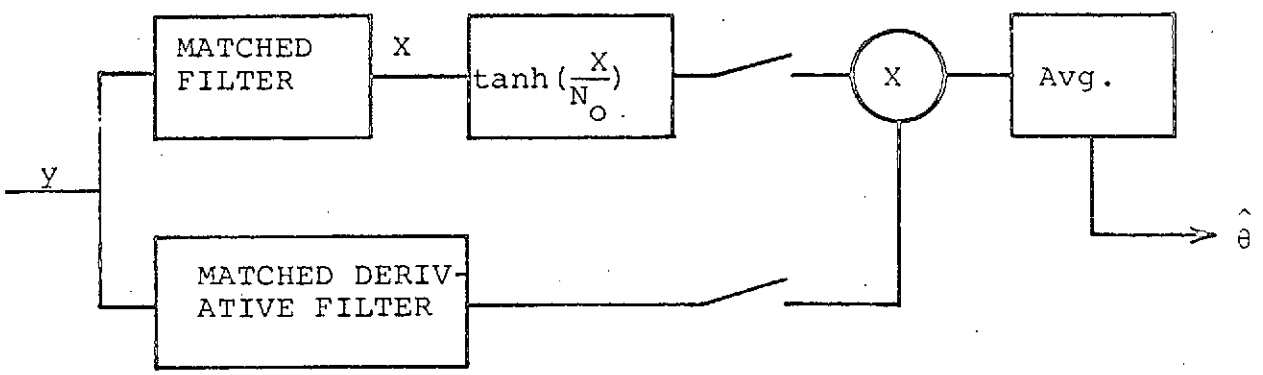

This configuration has some interesting properties. For high SNR, $\tanh\left(\frac{x}{N_o}\right)$ is a hard limiter, and the combination of the matched filter and nonlinearity is a bit detector. At low SNR, the detector is more like a difference of squares configuration. It should be noted that this linearized synchronizer does not work for square signals, because $s(t)$ is not differentiable. The bank-of-filters synchronizer works but is impractical. The option usually chosen is the early-late gate synchronizer described, in various forms by Simon [9], Stiffler [10], and others. A discrepancy also exists here between the well-known Wintz & Luecke results and the usual practical situation where the transmitted signal is a square signal passed through a filter. The result is an overlapping signal, not the non-overlapping version. A second difficulty stems from using the a priori probability for $P(\bar{a})$. Another approach is to use $P(\bar{a}_d)$ where $\bar{a}_d$ is the detected bit sequence. This gives rise to a hard limiter rather than a hyperbolic tangent, or an absolute value rather than a log cosh. It has been shown by Simon [9], that the absolute value early-late gate is better than the squared loop. This approach can also be used with the overlapping signal case, and the resulting configuration is much simpler.

B. ML Synchronizer for Binary Overlapping Symbols

Wang [11] has developed the maximum likelihood

synchronizer for generalized binary overlapping symbols. The synchronizer structure consists of matched filters, a transition detector and an accumulator. The form of the synchronizer does not lend itself to simple implementation. The results, however, are new, and provide some insight into the solution of problems with more practical waveforms than have been treated in the literature.

For the purpose of computer simulation the idealized overlapping NRZ waveform shown in Figure 5.1 was used. The analytical expression for the overlapping signal, $S_p(t)$, is also a function of $\alpha$, where $\alpha$ is defined as the overlapping parameter and is in the range from -0.5 to +0.5. The received signal waveforms are indicated by Figure 5.2(a) for the noiseless case, and by Figure 5.2(b) for the noisy case. The dotted line in the figure shows the individual overlapping symbol and the solid line is the actual received waveform.

The received signal is perturbed by an additive noise, $n(t)$, which is assumed to be a sample function from a Gaussian random process with zero mean and known variance. The input to the synchronizer is of the following form,

$$y(t) = S(t;\theta,A) + n(t), \qquad 0 \leq t < m \tag{5.2}$$

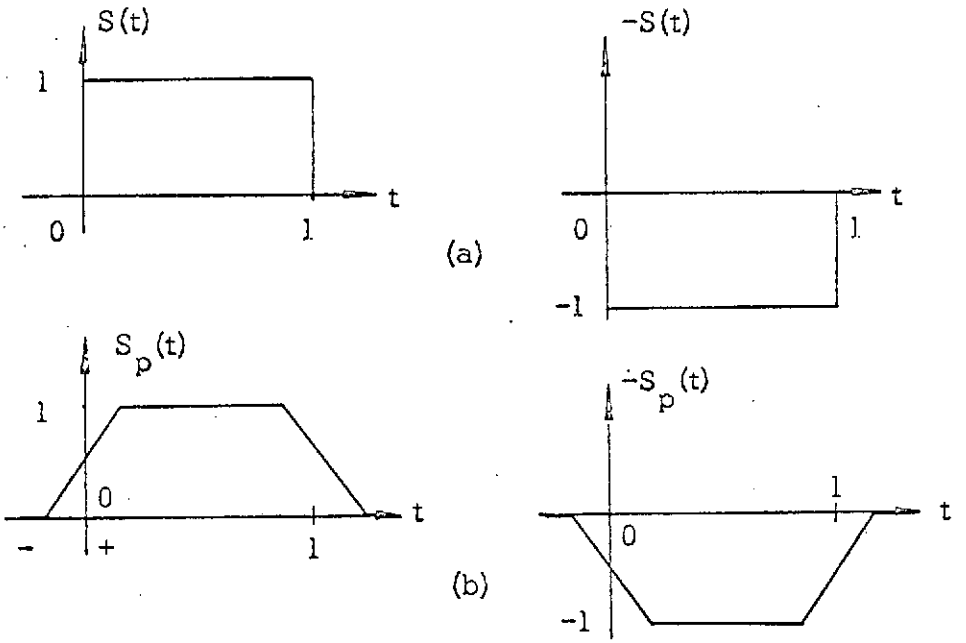


Fig. 5.1(a) Binary NRZ symbols
(b) Binary overlapping symbols

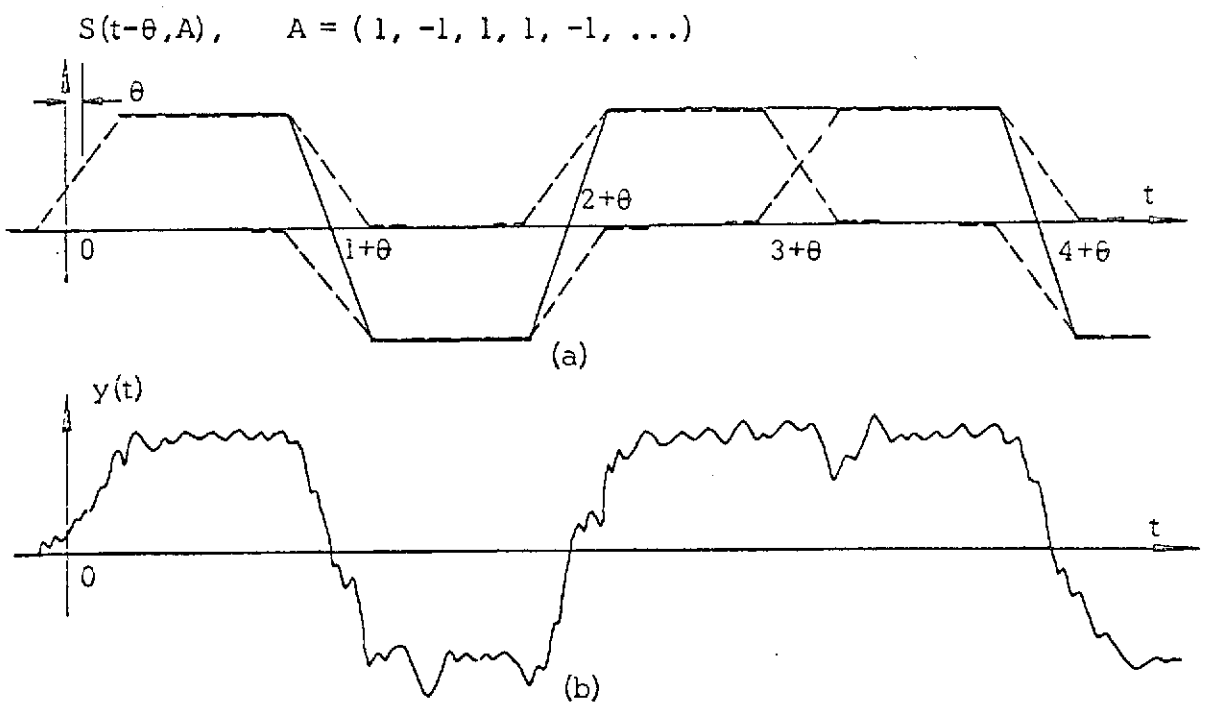


Fig. 5.2(a) Received signal without noise
(b) Received signal with noise

where $A = (a_1, a_2, \ldots, a_m)$,

$a_j$ = +1 or -1 with equal probability, and

$\theta$ = epoch to be estimated which is assumed uniformly distributed between -1/2 and +1/2.

1. Derivation of Optimum Synchronizer

In order to find the maximum likelihood (ML) solution, the conditional probability function $P(Y|\theta)$ is required. Owing to the presence of the random variable A, the following expression is considered.

$$P(Y|\theta) = \int_A P(Y|\theta,A)P(A)\, dA \tag{5.3}$$

We now find the conditional probability density function by using sampling approach, first taking N samples in each interval, and then letting the samples become dense, thus obtaining an integral form for $P(Y|\theta,A)$. For each sample i, $Y(i) = S(i;\theta,A) + n(i)$, $i=1,2,\ldots,mN$, where $n(i)$ is Gaussian distributed with zero mean and variance $B_oN$. The conditional joint pdf, $P(Y|\theta,A)$ for mN samples is written as:

$$P(Y|\theta,A) = \prod_{i=0}^{mN} (1/2\ B_oN)\ \exp\{-(1/2B_oN)[Y(i) - S(i;\theta,A)]^2\} \tag{5.4}$$

When N becomes very large, (5.4) can be written as an integral as follows,

$$P(Y|\theta,A) = K_1 \exp\left[-(1/2B_o) \int_0^m [y(t) - S(t;\theta,A)]^2 \, dt\right], \tag{5.5}$$

where $K_1$ is a constant. Because of the overlapping situation, the set of random variables $\{a_i\}$, j=1,2,...,m, are correlated with each other. Thus $P(Y|\theta,A)$ cannot be expressed as the product of the conditional pdf of individual symbols, namely, $P(Y|\theta,a_j)$, j-1,2,...,m. In order to proceed, we group the signal sequences as follows,

$$S(t;\theta,A) = \sum_{j=1}^{m-1} [a_j S_p(t-j;\theta) + a_{j+1} S_p(t-j+1;\theta)] \tag{5.6}$$

and integrate each interval from (j-1/2) to (j±1/2), so that (5.5) can be further simplified as follows:

$$P(Y|\theta,A) = K_1 \prod_{j=1}^{m-1} \exp\left[-(1/2B_o) \int_{j-1/2}^{j+1/2} [y(t) - a_j S_p(t-j;\theta) - a_{j+1} S_p(t-j-1;\theta)]^2 \, dt\right] \tag{5.7}$$

There are six terms to be considered if we expand out the above expression. However, three of them, involving the integration of squared terms, are actually constants. Hence their product can be combined with $K_1$ to form another constant $K_2$. Since $K_2$ is not a function of $\theta$, it will not enter into the maximizing process. We simply ignore this quantity for awhile. Note that if $\theta$ is also

assumed to be stationary, we can write $S(t;\theta) = S(t-\theta)$, for $-1/2 \leq \theta \leq 1/2$. Therefore, (5.7) is reduced to

$$P(Y|\theta,A) = \prod_{j=1}^{m-1} \exp\{a_j B_j(\theta) + a_{j+1} C_j(\theta) - a_j a_{j+1} D\} \qquad (5.8)$$

where

$$B_j(\theta) = (1/B_o) \int_{j-1/2}^{j+1/2} y(t) S_p(t-\theta-j)\, dt \qquad (5.9)$$

$$C_j(\theta) = (1/B_o) \int_{j-1/2}^{j+1/2} y(t) S_p(t-\theta-j-1)\, dt \qquad (5.10)$$

$$D = (1/B_o) \int_{j-1/2}^{j+1/2} S_p(t-\theta-j) S_p(t-\theta-j-1)\, dt \qquad (5.11)$$

D can be calculated immediately to be $\alpha/3$ and is not a function of $\theta$. The calculation of $B_j(\theta)$ and $C_j(\theta)$ proceeds as follows. When there is no transition in the interval $(j-1/2,\ j+1/2)$,

$$B_j(\theta) = ((a_j + a_{j+1})/2B_o)(1/2) \qquad (5.12)$$

$$C_j(\theta) = B_j(\theta). \qquad (5.13)$$

When there is a transition in the interval $(j-1/2,\ j+1/2)$, the situation is described by Figure 3.3 for the case $a_j = 1$, and $a_{j+1} = -1$. After integration, the values for $B_j(\theta)$ and $C_j(\theta)$ can be found as follows.

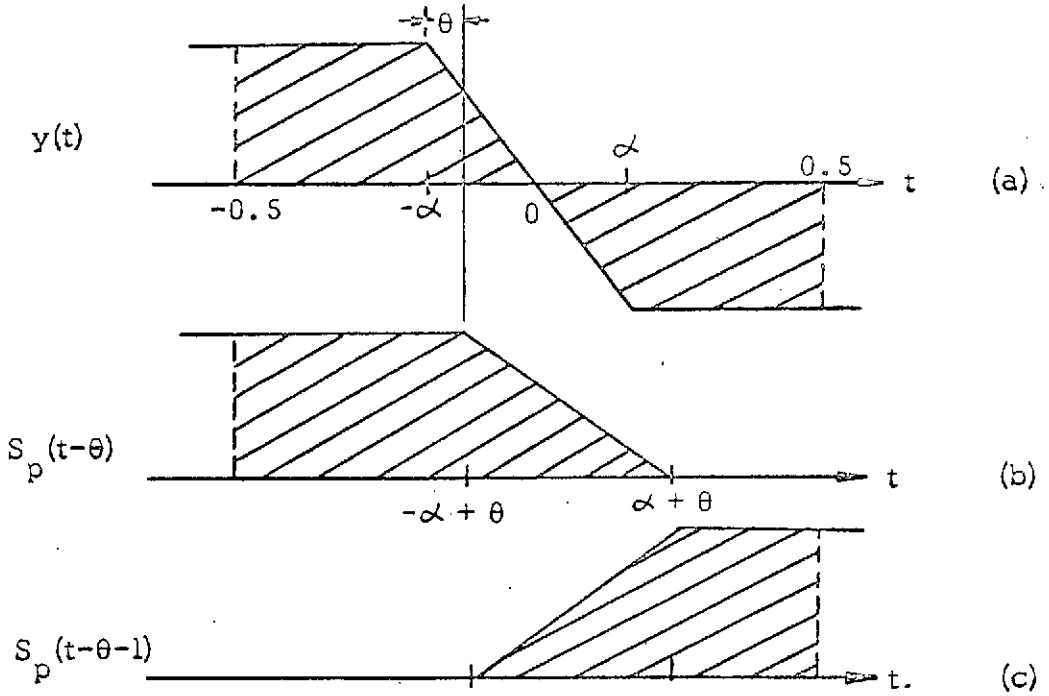


Fig. 3.3 On finding $B_j(\theta)$ and $C_j(\theta)$ when $\theta \geq 0$

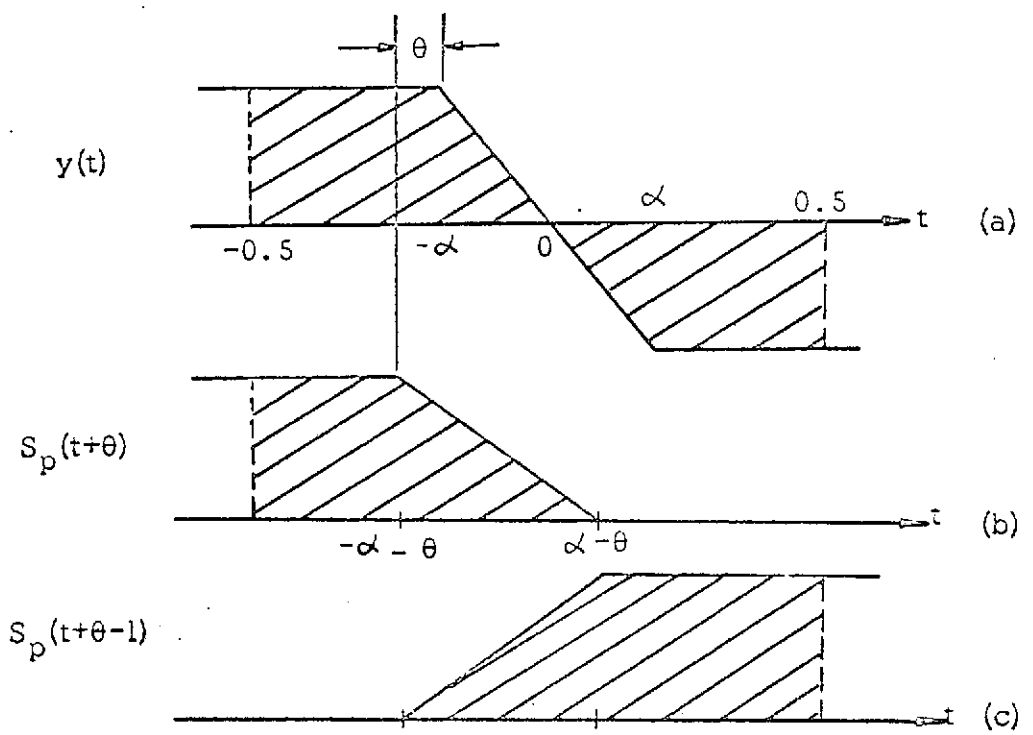


Fig. 3.4 On finding $B_j(\theta)$ and $C_j(\theta)$ when $\theta \leq 0$

$$B_j(\theta) = ((a_j - a_{j+1})/2B_o) \int_{-1/2}^{1/2} y(t)S(t-\theta)\,dt$$

$$= t_j \cdot (1/2 - (2\alpha/3) - (\theta^2/2\alpha) + (\theta^3/12\alpha^2)), \text{ for } \theta \geq 0 \tag{5.14}$$

$$C_j(\theta) = t_j \cdot (-1/2 - (2\alpha/3) + (\theta^2/2\alpha) - (\theta^3/12\alpha^2)), \text{ for } \theta \geq 0 \tag{5.15}$$

where $t_j = (a_j - a_{j+1})/2B_o$. For the case $\theta < 0$, it can be found that the values for $B_j(\theta)$ and $C_j(\theta)$ are the same as those indicated by (5.14) and (5.15) but with a different sign. Figure 5.4 shows the case for finding $B_j(\theta)$ and $C_j(\theta)$ when $\theta < 0$. In summary, $B_j(\theta)$ and $C_j(\theta)$ can be tabulated in Table 5.1:

Table 5.1 $B_j(\theta)$ and $C_j(\theta)$ for various $\theta$'s

| | | without transition | with transition |
|---|---|---|---|
| $\theta > 0$ | $B_j(\theta)$ | $(a_j + a_{j+1})/4B_o$ | $((a_j - a_{j+1})/2B_o)\ x$ |
| | $C_j(\theta)$ | $(a_j + a_{j+1})/4B_o$ | $((a_j - a_{j+1})/2B_o)(-x)$ |
| $\theta < 0$ | $B_j(\theta)$ | $(a_j + a_{j+1})/4B_o$ | $((a_j - a_{j+1})/2B_o)\ y$ |
| | $C_j(\theta)$ | $(a_j + a_{j+1})/4B_o$ | $((a_j - a_{j+1})/2B_o)(-y)$ |
| where $x = 1/2 - (2\alpha/3) - \theta^2/2\alpha + \theta^3/12\alpha^2$, $y = 1/2 - (2\alpha/3) - \theta^2/2 - \theta^3/12\alpha^2$. | | | |

The next problem is to maximize $\int P(Y|\theta,A)P(A)\,dA$ to obtain the optimum estimate. Owing to the overlapping situation, the exponential term in (5.8) consists of both the symbol $a_j$ and the following symbol $a_{j+1}$. The averaging process is therefore of a recursive nature. Further, the random variable $a_j$ is equally likely to be +1 or -1 so that four different cases should included. For convenience, let

$$Q(\theta,a_j,a_{j+1}) = \exp(a_jB_j(\theta) + a_{j+1}C_j(\theta) - a_ja_{j+1}D), \quad (5.16)$$

and let

$Q(\theta,a_j=1,a_{j+1}=1)$ be represented by simply $Q(1,1)$. If we use the subscripts 0 and 1 to represent the symbol -1 and +1, respectively, the probability of (j+1)th stage can be written as a function of the jth stage as follows:

$$P_1(j+1) = P(Y|\theta,j+1,1) = P(Y|\theta,j,-1)Q(-1,1) + P(Y|\theta,j,1)Q(1,1) \quad (5.17a)$$

$$P_0(j+1) = P(Y|\theta,j+1,-1) = P(Y|\theta,j,-1)Q(-1,-1) + P(Y|\theta,j,1)Q(1,-1) \quad (5.17b)$$

Or, if we write the above expressions in matrix form,

$$\begin{pmatrix} P_0(j+1) \\ P_1(j+1) \end{pmatrix} = \begin{pmatrix} Q(-1,-1) & Q(1,-1) \\ Q(-1,1) & Q(1,1) \end{pmatrix} \begin{pmatrix} P_0(j) \\ P_1(j) \end{pmatrix} \quad (5.18)$$

The next step is to compute the average of $P_0(j+1)$ and $P_1(j+1)$ using the following equation:

$$\begin{pmatrix} P_2(j+1) \\ \\ P_3(j+1) \end{pmatrix} = (1/2)\begin{pmatrix} 1 & 1 \\ \\ 1 & -1 \end{pmatrix}\begin{pmatrix} P_0(j+1) \\ \\ P_1(j+1) \end{pmatrix}$$

$$= (1/2)\begin{pmatrix} 1 & 1 \\ \\ 1 & 1 \end{pmatrix}\begin{pmatrix} Q(-1,-1) & Q(1,-1) \\ \\ Q(-1,1) & Q(1,1) \end{pmatrix}\begin{pmatrix} 1/2 & 1/2 \\ \\ 1/2 & 1/2 \end{pmatrix}\begin{pmatrix} P_2(j) \\ \\ P_3(j) \end{pmatrix} \quad (5.19)$$

To write (5.19) in a matrix form, we have

$$P(j+1) = H_j(\theta)P(j) \quad (5.20)$$

where $H_j(\theta)$ is a two by two matrix having the following elements,

$$\begin{aligned} h_{11}(\theta) &= e^{-C_j}\cosh(D+B_j) + e^{C_j}\cosh(B_j-D) \\ h_{12}(\theta) &= -e^{-C_j}\sinh(D+B_j) + e^{C_j}\sinh(D-B_j) \\ h_{21}(\theta) &= e^{C_j}\cosh(D+B_j) - e^{-C_j}\cosh(D-B_j) \\ h_{22}(\theta) &= -e^{C_j}\sinh(D+B_j) - e^{+C_j}\sinh(D-B_j) \end{aligned} \quad (5.21)$$

The associated synchronizer structure is shown in the next section.

2. The Synchronizer Structure

The ML synchronizer structure consists of matched filter, a transistion detector, a weighting function and a feedback circuit. To obtain the maximum value of the

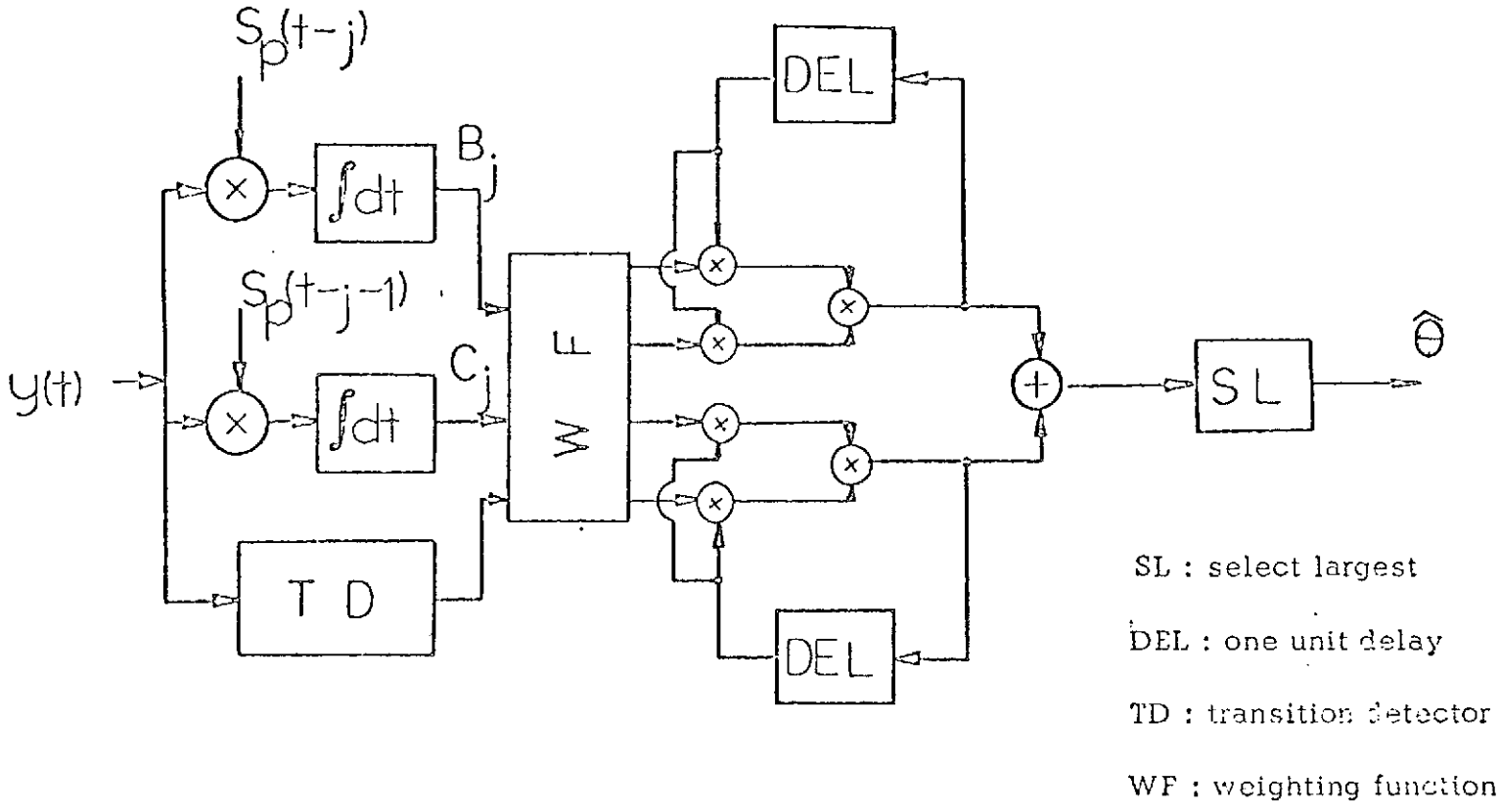


Fig. 5.5 ML Synchronizer for Binary Overlapping Signals

density function for a given received y(t), y(t) is first correlated with the overlapping symbol $S_p(t)$ and $S_p(t-1)$ separately in the time interval (1/2, 3/2). The transition detector is a device which examines $a_j$ and $a_{j+1}$ in the presence of noise, and records an output $t_j$ according to the following rules:

$$\text{If } a_j = a_{j+1}, \quad t_j = (a_j + a_{j+1})/2.$$

$$\text{If } a_j \neq a_{j+1}, \quad t_j = (a_j - a_{j+1})/2.$$

The output of the matched filters and the transition detector are then passed to a weighting function which computes the four Q-functions. Then the conditional probability density function for each stage is calculated and stored. The feedback circuitry is used here to generate the conditional probability density function recursively. At the end of the mth symbol, the output statistics in each stage are compared, and the largest statistic is announced as the estimate of the correct synchronization position. The maximum likelihood synchronizer consists of a bank of devices followed by a maximum value selector. In a manner similar to that employed without overlapping symbols, a single line synchronizer can be developed for continuous $S(\varepsilon)$. The correlator output can be recognized as a transition detector. The exponential form of the nonlinearities can

again be recognized as a result of using the a priori probability $P(\bar{a})$ in the derivation. If $P(\bar{a}_d)$, the probability after detection, is used, the result is a detector used to control a matched derivative filter. This results in a much simpler structure and is in fairly close correspondence with many existing units.

3. Monte Carlo Simulation Program and Results

In order to find the exact value of the conditional probability density function $P(Y|\theta)$, we again examine (5.7):

$$P(Y|\theta,A) = \prod_{i=1}^{m-1} K_1 \exp\left[-(1/2B_0) \int_{i-1/2}^{i+1/2} [y(t) - a_i S_p(t-i-\theta) - a_{i+1} S_p(t-i-1-\theta)^2 \, dt\right]$$

$$= \prod_{i=1}^{m-1} K_1 \exp\{K_5 + a_i B_i(\theta) + a_{i+1} C_i(\theta) - a_i a_{i+1} D\}. \tag{5.23}$$

where $$K_1 = 1/\sqrt{2\pi B_0}. \tag{5.24}$$

$K_5$ can be written as the sum of there terms:

$$K_5 = K_2 + K_3(\theta) + K_4(\theta) \tag{5.25}$$

where $$K_2 = -(1/2B_0) \int_{i-1/2}^{i+1/2} y^2(t) \, dt$$

$$= \begin{cases} -(3 - 4\alpha)/6B_0, & \text{if there is a transition} \\ -(1/2B_0), & \text{if there is no transition} \end{cases} \tag{5.26}$$

$$K_3(\theta) = -(1/2B_o) \int_{i-1/2}^{i+1/2} S_p^{\,2}(t-\theta-i)\, dt$$

$$= -(1/2B_o) \int_{1/2}^{1/2} S^2(t-\theta)\, dt$$

$$= -(1/2B_o)\ [-\alpha/3 + 1/2 + \theta] \qquad (5.27)$$

$$K_4(\theta) = -(1/2B_o) \int_{1/2}^{1/2} S^2(t-\theta-1)\, dt$$

$$= -(1/2B_o)\ [-\alpha/3 + 1/2 - \theta] \qquad (5.28)$$

At first glance, $K_3(\theta)$ and $K_4(\theta)$ are functions of $\theta$ so that they ought to be included in Section 3.B. However, their sum indicates that $K_5$ is not a function of $\theta$. That is

$$K_5 = K_2 + K_3(\theta) + K_4(\theta)$$

$$= \begin{cases} -((1 - 2\alpha)/B_o), & \text{if there is a transition} \\ -((3 - \alpha)/{}_3B_o), & \text{if there is no transition} \end{cases} \qquad (5.29)$$

The input bit stream for the simulation program is generated by a uniform random number generator. The description of this subroutine is given in Appendix A. The signal-to-noise

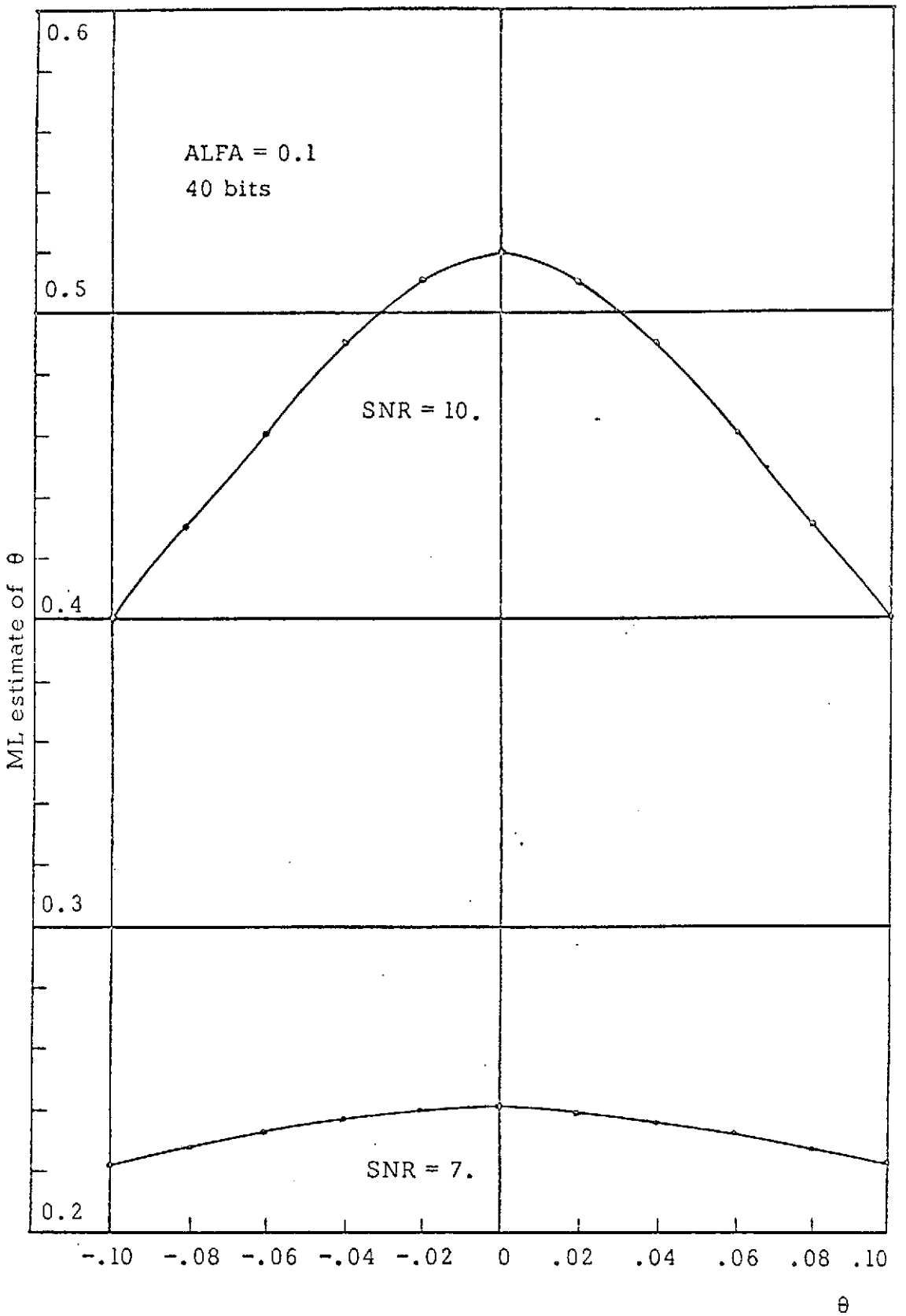


Fig. 5.7a Results of the ML Synchronization Program

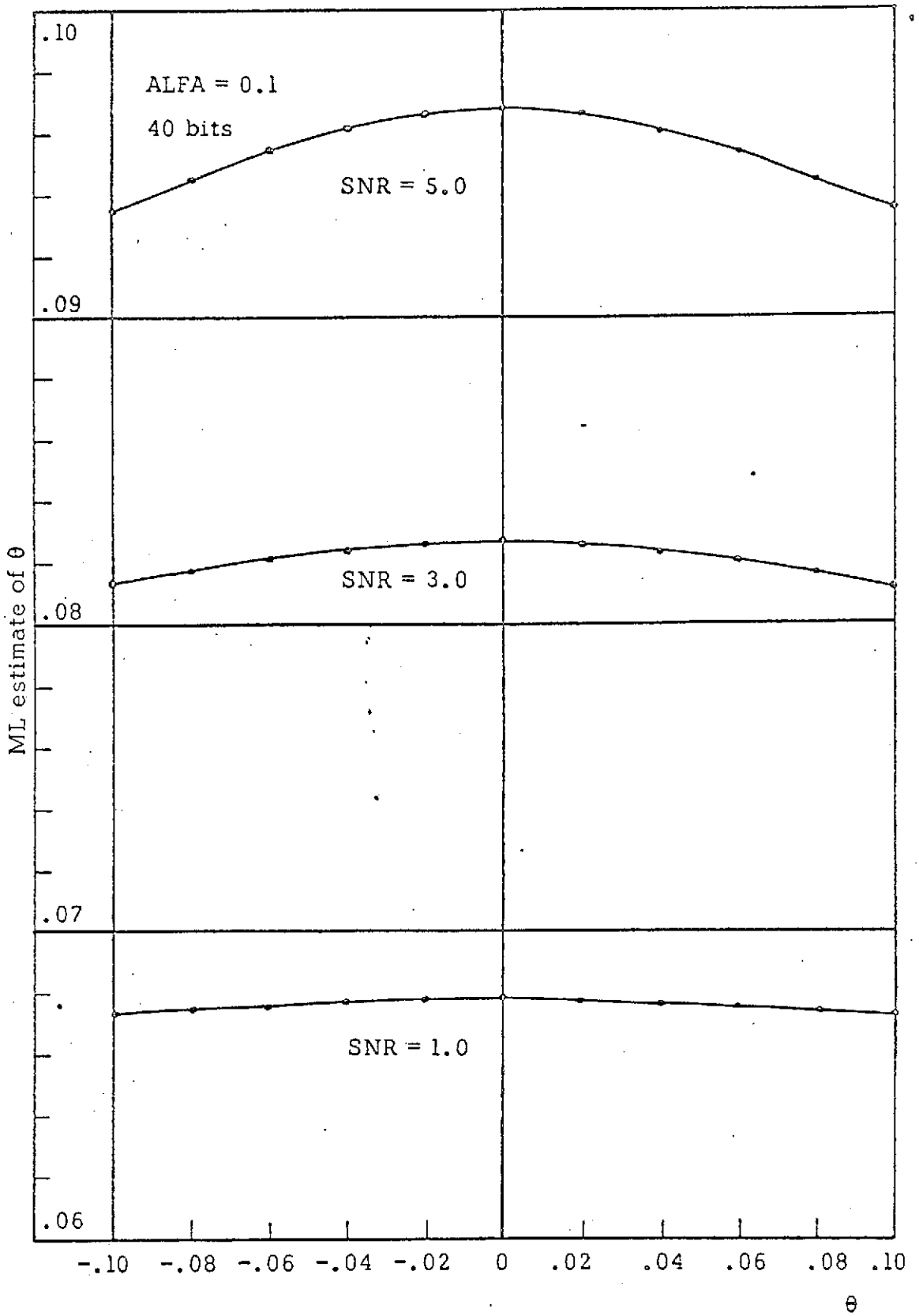


Fig. 5.7b Results of the ML Synchronization Program

ratio (SNR) in the program is the power ratio indicated by numbers. $\theta$ in the simulation program is the true value. For 40 bits as the input data to the ML synchronizer, the probability density function versus different $\theta$ are plotted in Figure 5.7, using SNR as a parameter. The graphs appear to be nearly Gaussianly distributed with center around $\theta = 0$. At high SNR, the curve tends to peak up at the origin and to flatten out rapidly as the SNR decreases.

## C. Analysis for Bandlimited Overlapping Signals

The received signal in satellite telemetry has some overlap between bits that may be caused by the transmitter filter, the channel or by the receiver filter. In most cases the most severe bandlimiting is due to the receiver IF section, but even here the symbols are usually contained within two bit periods.

Suppose we receive the signal

$$y(t) = \sum_{-\infty}^{\infty} a_n \, s(t-\theta-nT) + n(t) \ ,$$

pass it through an ideal low-pass filter of bandwidth B, and let the output be given by $y^*(t)$, where

$$y^*(t) = \sum_{-\infty}^{\infty} b_n(t) + n_L(t) .$$

The conditional pdf of $y^*(t)$, given sync error $\theta$ and signal sequence A, is given as

$$P(y^*(Y)\,|\,\theta,A) = K_1 \exp\{-(1/2B_o) \sum_{n=1}^{N} [y^*(n) - \sum_{k=1}^{N} a_k S_p(n-k-\theta)]^2\} \tag{6.4}$$

We now use the fact that the overlapping signals with synchronization error $\theta$, can be approximated by the following linear relationship:

$$S(t - \theta) = S(t) - \theta\, S'(t) \tag{6.5}$$

The associated waveforms are shown in Figure 6.1. For small $\theta$, the difference between the two curves is small enough to be neglected. Using this approximation in the conditional probability density function,

$$P(y^*(t)\,|\,\theta,A) = K_1 \exp\{-(1/2B_o) \sum_{n=1}^{N} [(y^*(n) - \sum_{k=1}^{N} a_k S_p(n-k)) + \theta \sum_{k=1}^{N} a_k S_p'(n-k)]^2\} \tag{6.6}$$

To find the optimum estimate of $\theta$, we set

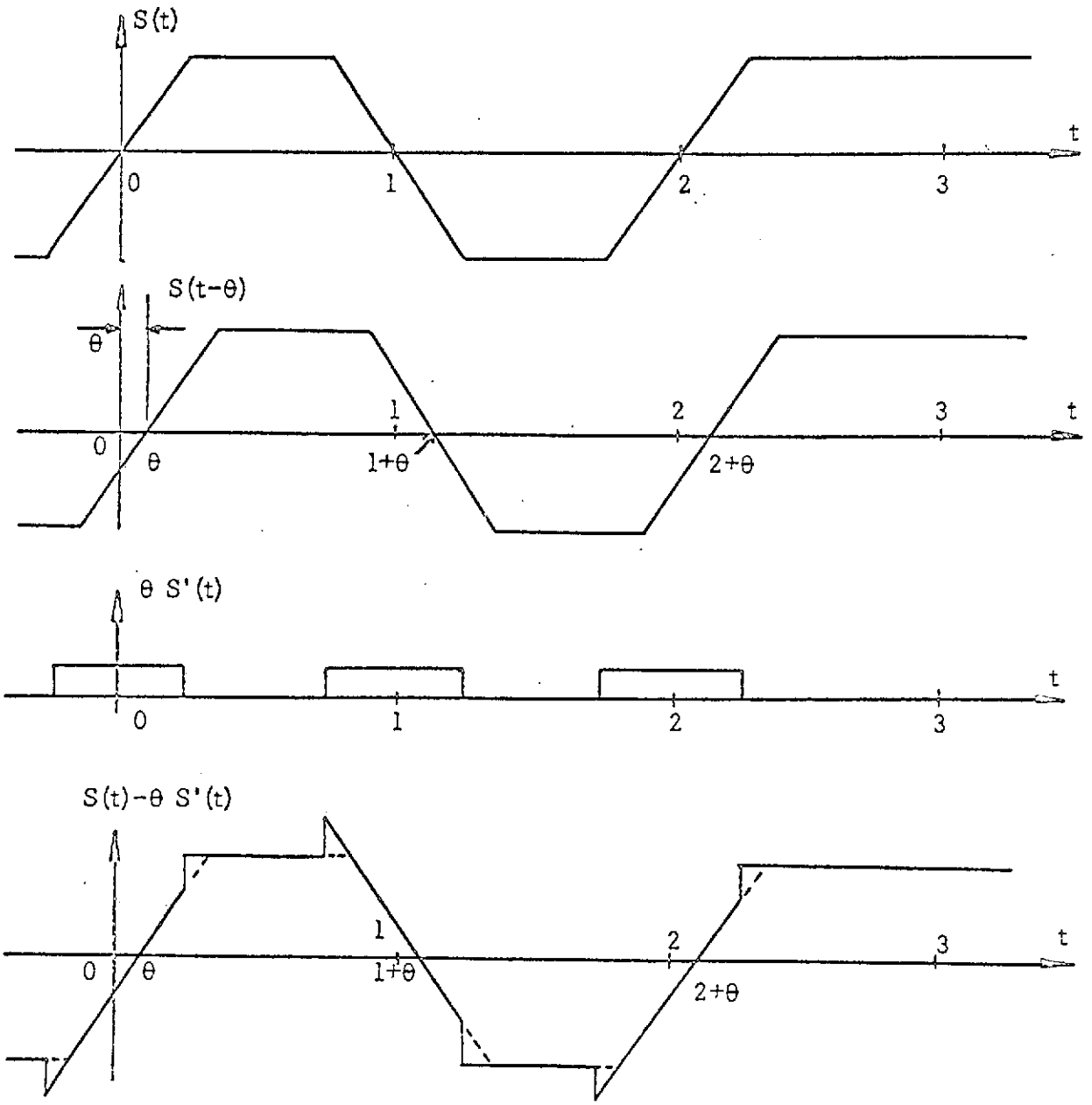


Fig. 6.1 Linear approximation of the overlapping signal

$$\left.\frac{\delta \ln P(y^*(t)\,|\,\theta,A)}{\delta\theta}\right|_{\theta = \hat{\theta}_{ML}} = 0$$

Thus,

$$\sum_{n=1}^{N} [y^*(n) - \sum_{k=1}^{N} a_k S_p(n-k) + \theta \sum_{k=1}^{N} a_k S_p'(n-k)].$$

$$\left.\sum_{k=1}^{N} a_k S_p'(n-k)\right|_{\theta = \hat{\theta}_{ML}} = 0. \qquad (6.7)$$

Solving for $\theta$, we find the following result:

$$\theta_{ML} = -\sum_{n=1}^{N} \frac{[y^*(n) - \sum_{k=1}^{N} a_k S_p(n-k)][\sum_{k=1}^{N} a_k S_p'(n-k)]}{\sum_{k=1}^{N}\sum_{j=1}^{N} a_k a_j S_p'(n-k) S_p'(n-j)} \qquad (6.8)$$

$$= K \sum_{n=1}^{N} [y^*(n) - \sum_{k=1}^{N} a_k S_p(n-k)][\sum_{k=1}^{N} a_k S_p'(n-k)] \qquad (6.9)$$

The above derivation leads to a synchronizer which is roughly sketched in Figure 6.2.

The received signal is first passed through a detector to form the original overlapping signal and then the derivative of the signal. Meanwhile, it is bandlimited by passing through a low-pass filter with bandwidth 2B. After forming the signal, we subtract the two waveforms, and the

difference is further multiplied by the derivative of the original signal, d(t). The final block is an accumulator. The operation of the synchronizer is shown in Figure 6.3(a) and 6.3(b). With the input signal having different delays, the estimated values of θ's are shown as functions of θ's.

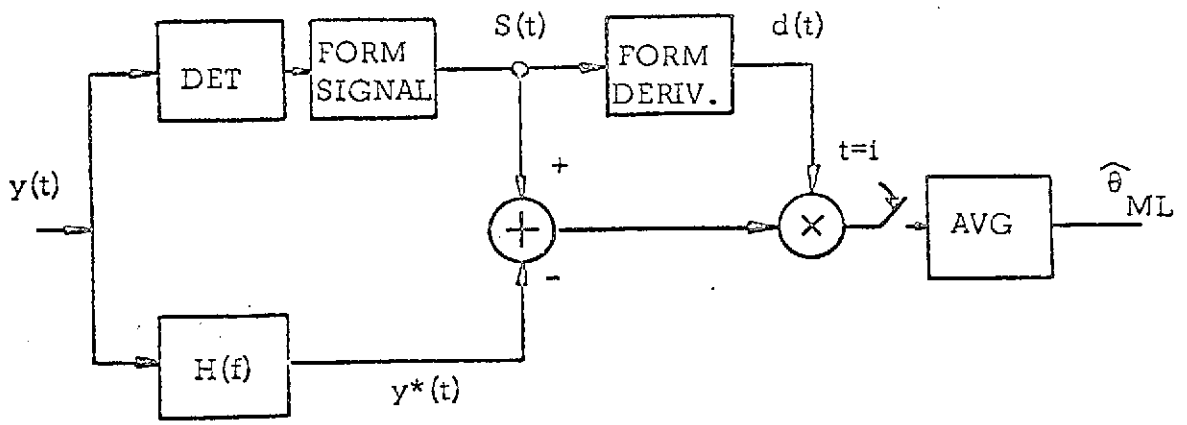


Fig. 6.2. Block diagram of the suboptimum synchronizer

Furthermore, the detector portion is replaced by the DD detector investigated in Chapter VI. The overall block diagram is given in Figure 6.4. In order to simulate this system, we need to have the theoretical expression of the bandlimited signal by Fourier analysis and the bandlimited noise by autocorrelation analysis. This will be considered in the next section.

1. Bandlimiting and Sampling of the Overlapping Signals

To find the output of the filter, we shall first find the Fourier transform of the overlapping symbol. It is

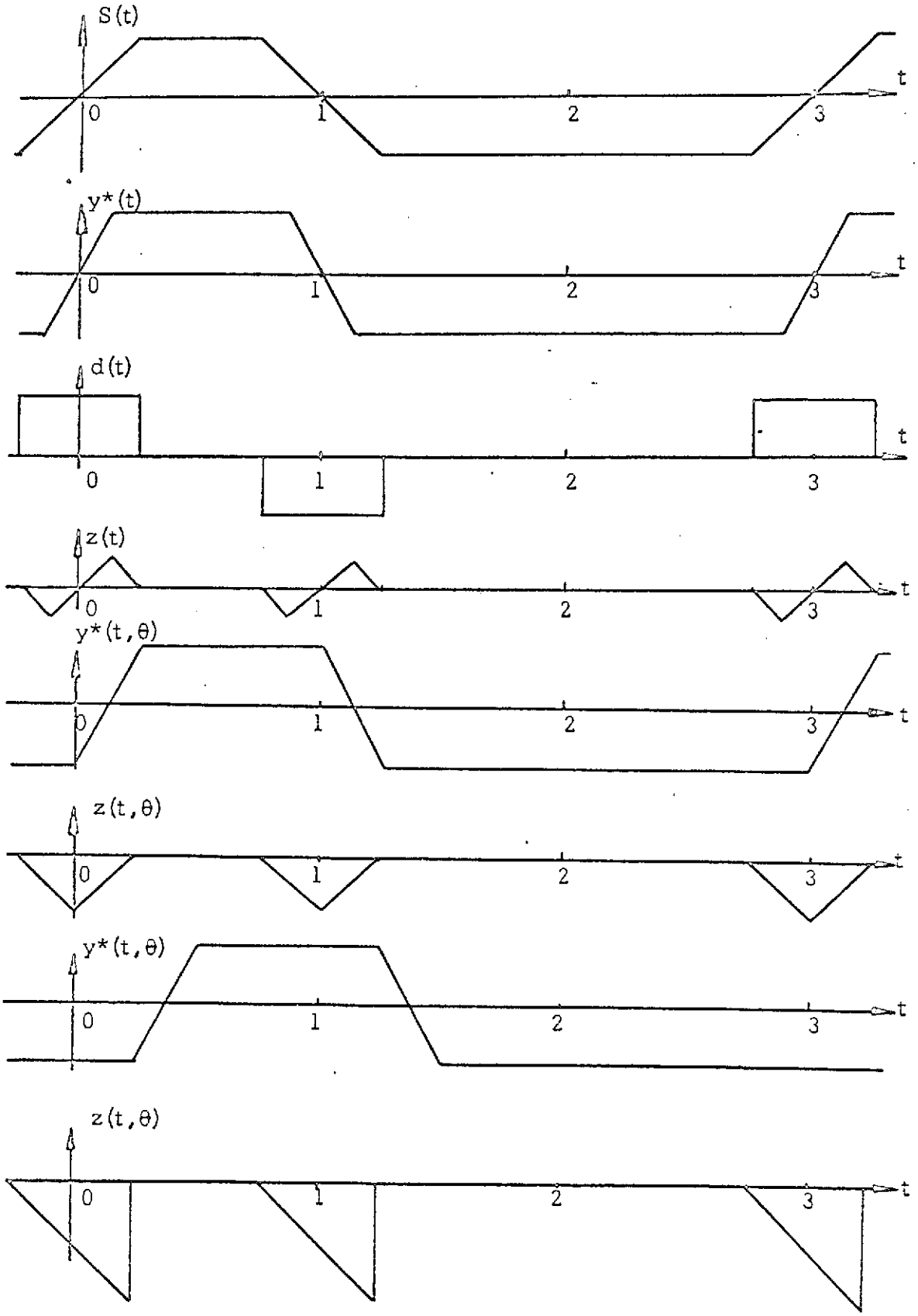


Fig. 6.3(a) Output waveforms of the suboptimum synchronizer for $\theta \geqslant 0$

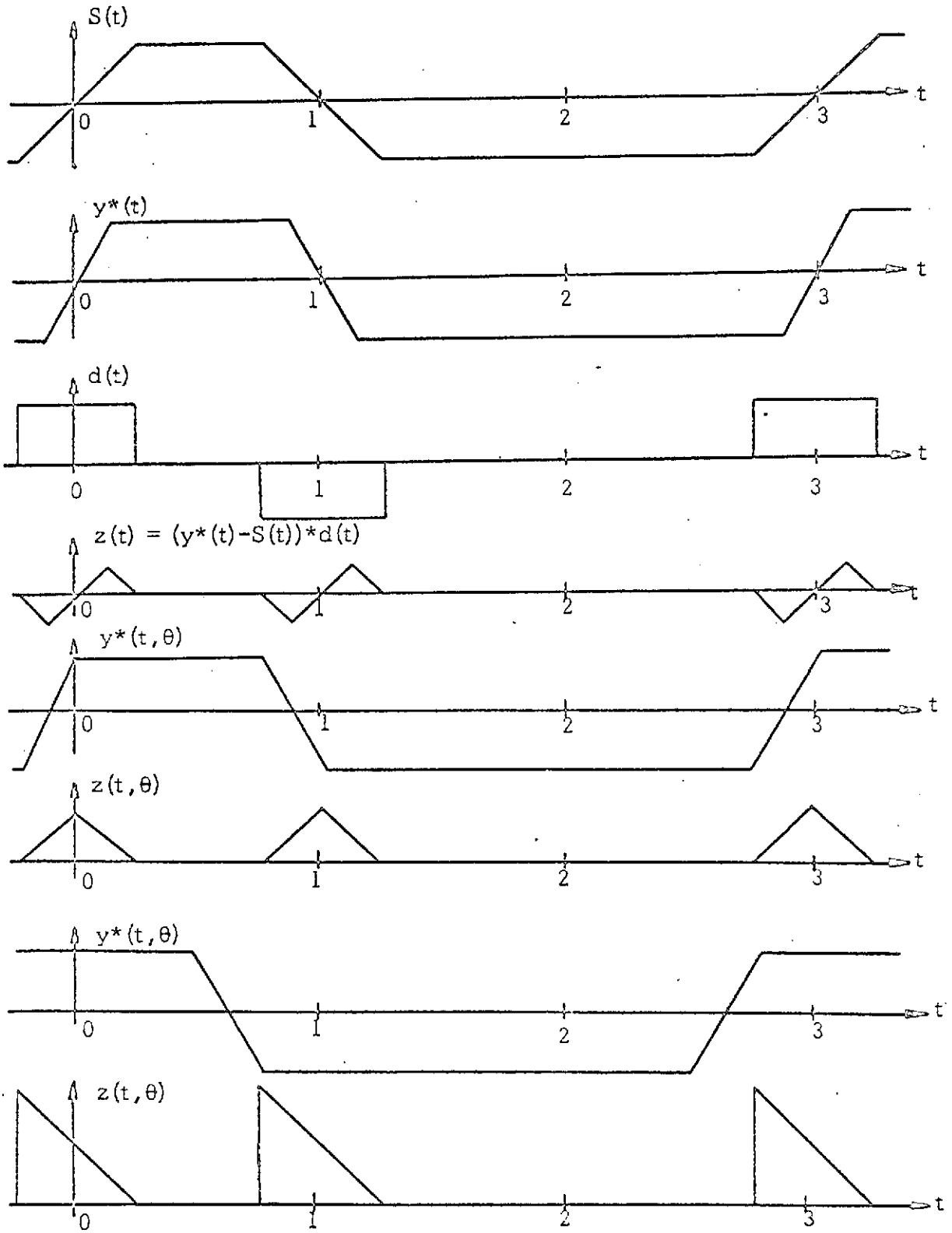


Fig. 6.3(b) Output waveforms of the suboptimum synchronizer for $\theta \leqslant 0$

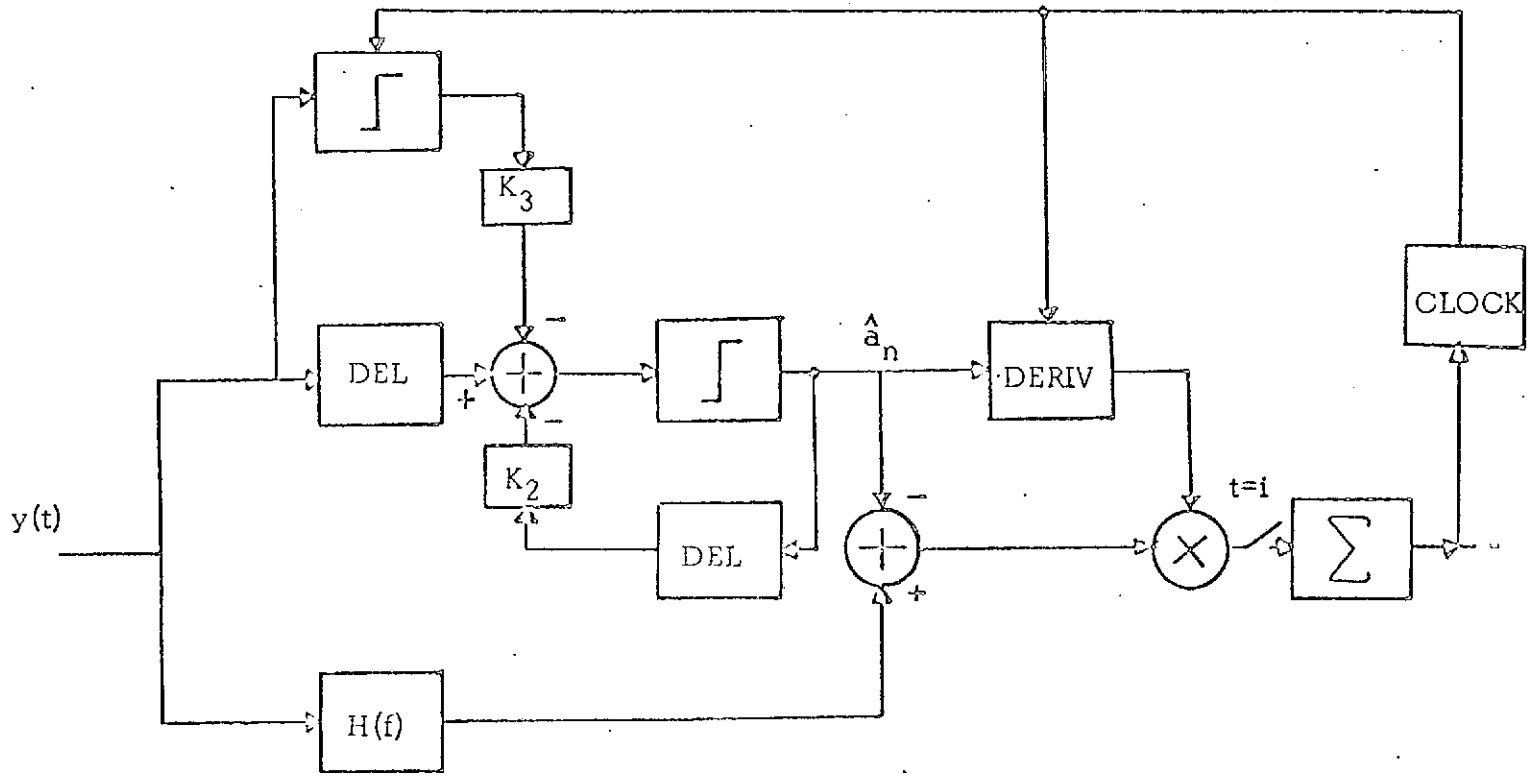


Fig. 6.4 Suboptimum synchronizer structure

that if the symbol is differentiated with respect to time twice, a sequence of impulses can be obtained. The transform of the impulses is readily found. Let the symbol be centered at origin and be called f(t). It is evident from Figure 6.5(c) that

$$\frac{d^2f}{dt^2} = (1/2\alpha)[\delta(t+1/2+\alpha) - \delta(t+1/2-\alpha) - \delta(t-1/2+\alpha) + \delta(t-1/2-\alpha)] \qquad (6.10)$$

Using the Fourier time shift theorem, we have

$$(jw)^2F(w) = (1/2\alpha)\left[\exp[jw(1/2+\alpha)] - \exp[jw(1/2-\alpha)] - \exp[-jw(1/2-\alpha)] + \exp[jw(1/2+\alpha)]\right]$$

Thus,

$$F(w) = (1/\alpha w^2)[\cos(1/2-\alpha)w - \cos(1/2+\alpha)w] \qquad (6.11)$$

The time shift theorem is used again to obtain $S_p(w)$, the Fourier transform of the overlapping symbol, $S_p(t)$.

$$S_p(w) = (1/\alpha w^2)[\cos(1/2-\alpha)w - \cos(1/2+\alpha)w]\ \exp(-jw(1/2))$$

$$S_p(w) = (1/\alpha w^2)\ 2\ \sin(w/2)\ \sin(\alpha w) \cdot \exp(-jw/2)$$

$$= \mathrm{Sa}(w/2)\ \mathrm{Sa}(\alpha w) \cdot \exp(-jw/2), \qquad (6.12)$$

where $\mathrm{Sa}(x) = \sin x/x.$

Let the output of the filter be

$$y^*(t) = \sum_{n=1}^{N} b_n(t) + n_1(t).$$

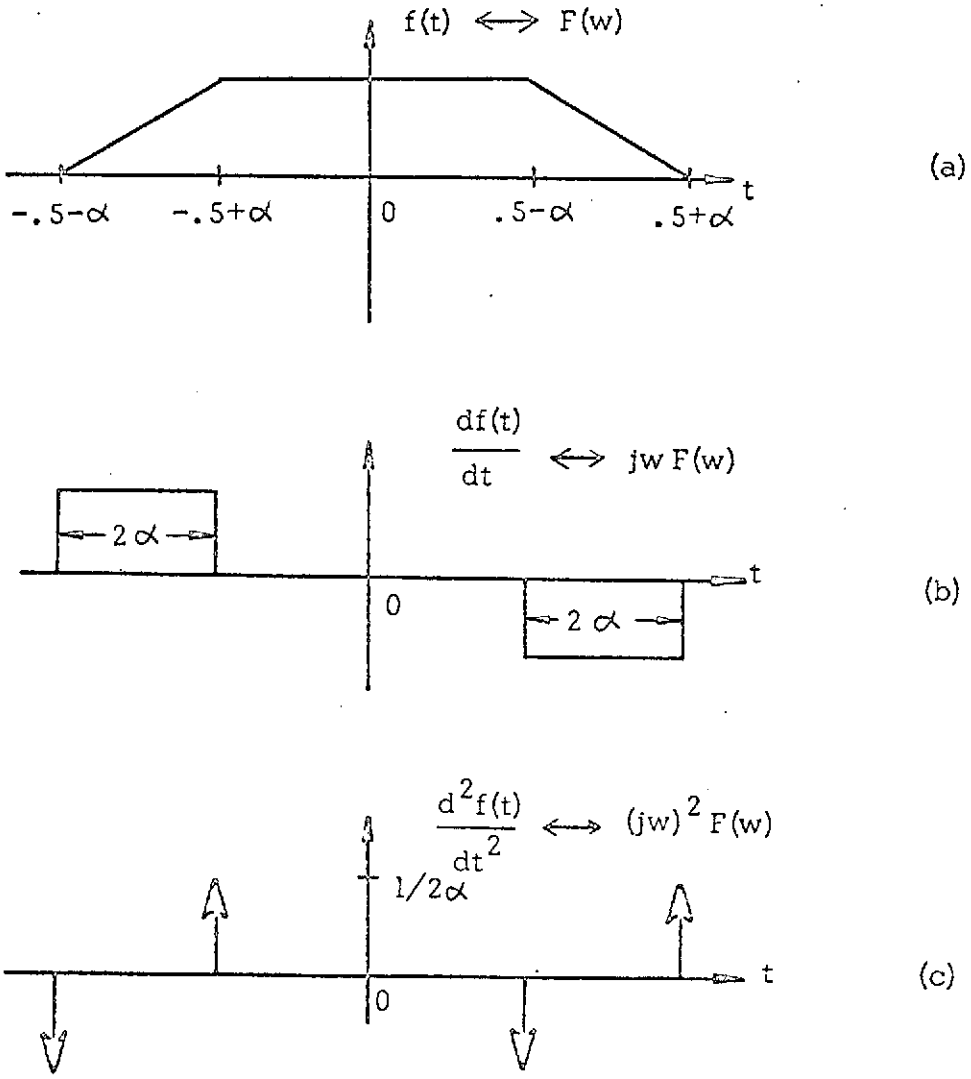


Fig. 6.5 Fourier transform of a trapezoidal function f(t)

Then the Fourier transform of the nth bit is

$$B_n(f) = \begin{cases} a_n Sa(\pi f)\ Sa(2\pi\alpha f) \cdot \exp(-j\pi f(1+2n)) & -B \le f \le B \\ 0, & \text{elsewhere} \end{cases} \qquad (6.13)$$

The time response $b_n(t)$ is

$$b_n(t) = \int_{-B}^{B} B_n(f) \cdot \exp(j2\pi ft)\, df \qquad (6.14)$$

$$= \int_{-B}^{B} a_n Sa(\pi f)\ Sa(2\pi\alpha f) \cdot \exp(-j\pi f(1+2n-2t))\, df$$

Substituting $\pi f = x$, we have

$$b_n(t) = a_n(2/\pi) \int_{0}^{\pi B} Sa(x)\ Sa(2\pi\alpha x) \cos(1+2n-2t)x\, dx \qquad (6.15)$$

The response of the sample due to an infinite bit train can be expressed as

$$y^*(t) = \sum_{n=-\infty}^{\infty} b_n(t) + n_1(t)$$

$$= a_o(2/\pi) \int_{0}^{\pi B} Sa(x)\ Sa(2\alpha x) \cos(1-2t)x\, dx$$

$$+ \sum_{n=-\infty}^{\infty} a_n(2/\pi) \int_{0}^{\pi B} Sa(x)\ Sa(2\alpha x) \cos(1+2n-25)x\, dx$$

$$+ n_1(t) \qquad (6.16)$$

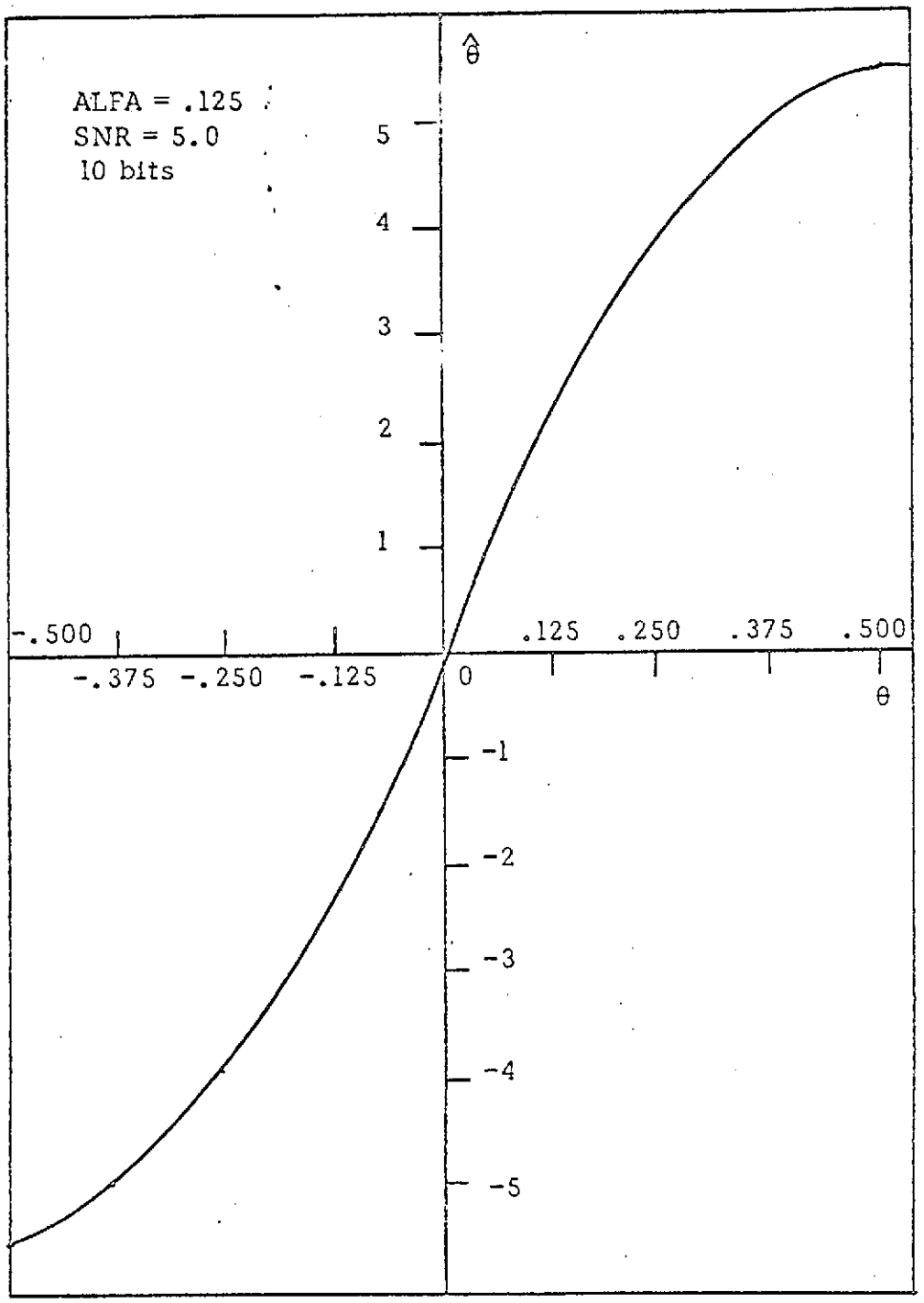


Fig. 6.8 Results of the suboptimum synchronizer simulation program

The first term is the desired signal and is peaked at t = 1/2, for B $\leq$ 1. The second term is the intersymbol interference due to bandlimiting the signals. Thus, sampled at t = 1/2, the response can be simplified to give

$$y^*(t=1/2) = a_0 S(B,0) + \sum_{n=-\infty}^{\infty} a_n S(B,n) + n_1(t) \qquad (6.17)$$

where $$S(B,0) = (2/\pi) \int_0^{\pi B} Sa(x)\ Sa(2\alpha x)\ dx$$

$$S(B,n) = (2/\pi) \int_0^{\pi B} Sa(x)\ Sa(2\alpha x)\ \cos(2nx)\ dx$$

The filter noise has the variance

$$\sigma^2 = \frac{N_0}{2} \int_{-B}^{B} |H(t)|^2\ df = N_0 B$$

2. Simulation Results

A program was written to evaluate the performance of the synchronizer developed above. One sample run of the program is presented here, using 10 random bits as the input data stream, with SNR of 5 and an overlap $\alpha$ = .25.

D. Synchronizer for Overlapping Split-Phase Signals

1. Bandlimiting and Sampling

Using the same technique as in Section B, the Fourier

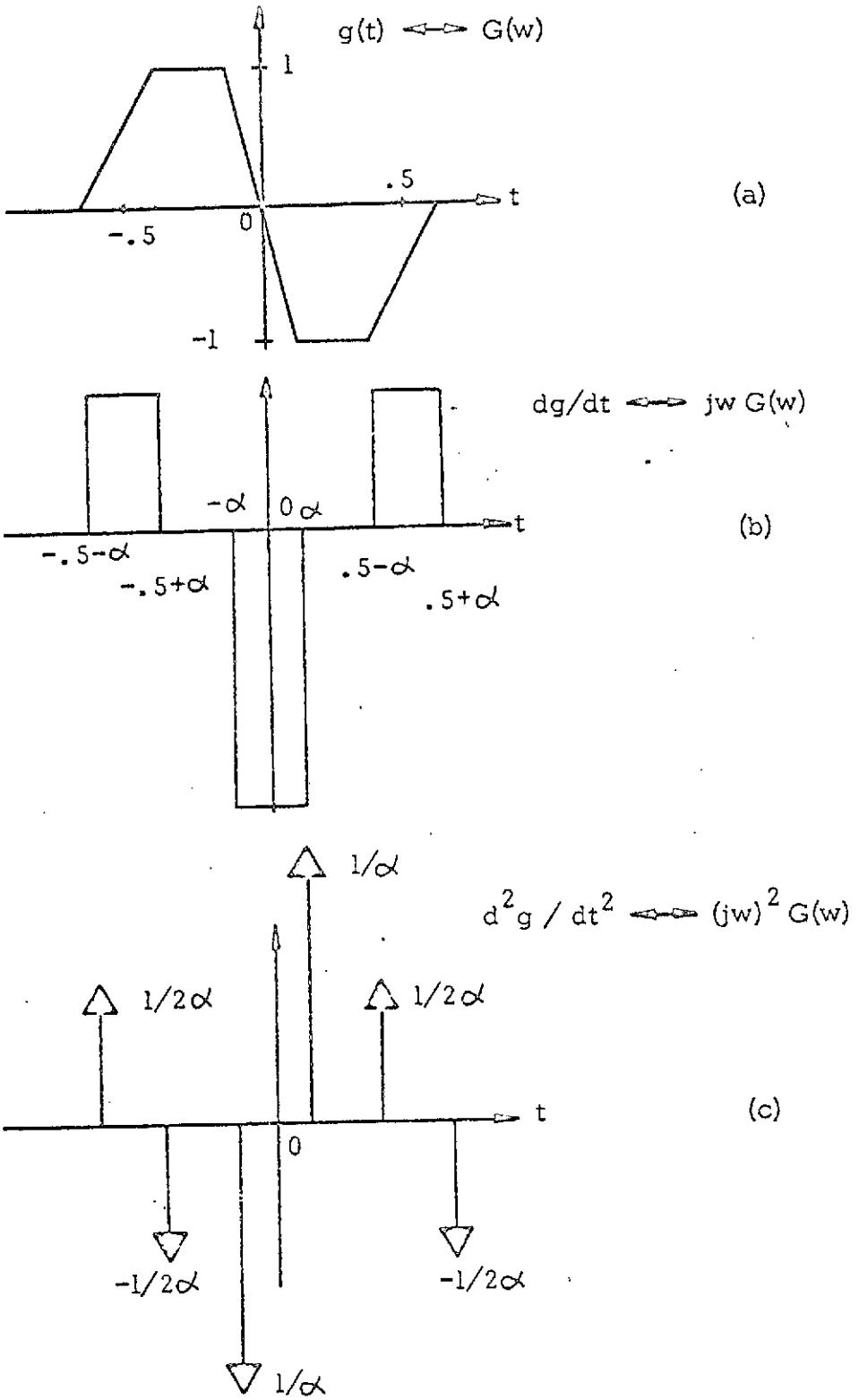


Fig.6.9 Fourier transform of a overlapping split-phase symbol

transform of the overlapping split phase (Sϕ) symbol g(t) as shown in Figure 6.9 is written as

$$\frac{d^2g}{dt^2} = (1/2\alpha)[\delta(t+1/2+\alpha) - \delta(t+1/2-\alpha) + \delta(t-1/2+\alpha) - \delta(t-1/2-\alpha)] + (1/\alpha)[-\delta(t+\alpha) + \delta(t-\alpha)] \quad (6.20)$$

Thus, using the transform pairs, we have

$$\begin{aligned}(jw)^2G(w) &= (1/2\alpha)[\exp(jw(1/2+\alpha)) - \exp(+jw(1/2-\alpha)) \\ &\quad + \exp(-jw(1/2-\alpha)) - \exp(-jw(1/2+\alpha))] \\ &\quad + (1/\alpha)[-\exp(jw\alpha) + \exp(-jw\alpha)] \\ &= (j/\alpha)[\sin(1/2+\alpha)w - \sin(1/2-\alpha)w] - (2j/\alpha)\cdot \\ &\quad \sin(\alpha w)\cdot \\ &= (2j/\alpha)[\cos(w/2)\ \sin(\alpha w) - \sin(\alpha w)]. \quad (6.21)\end{aligned}$$

Thus, $G(w) = 2j[\sin(\alpha w)/\alpha w^2]\ [1 - \cos(w/2)]$ (6.22)

Then the Fourier transform of the overlapping Sϕ symbol, $S_\phi(t)$, is

$$S_\phi(w) = G(w)\ \exp(-jw/2) \quad (6.23)$$

Let $w = 2\pi f \triangleq 2x$,

$$\begin{aligned}S_\phi(f) &= (j/x)(\sin(2\alpha x)/2\alpha x)(1 - \cos x)\ \exp(-jx) \\ &= j\ \mathrm{Sa}(2\alpha x)[(1 - \cos x)/x]\ \exp(-jx) \quad (6.24)\end{aligned}$$

If the output of the LPF is

$$y_\phi^*(t) = \sum_{n=-\infty}^{\infty} b_n(t) + n_1(t),$$

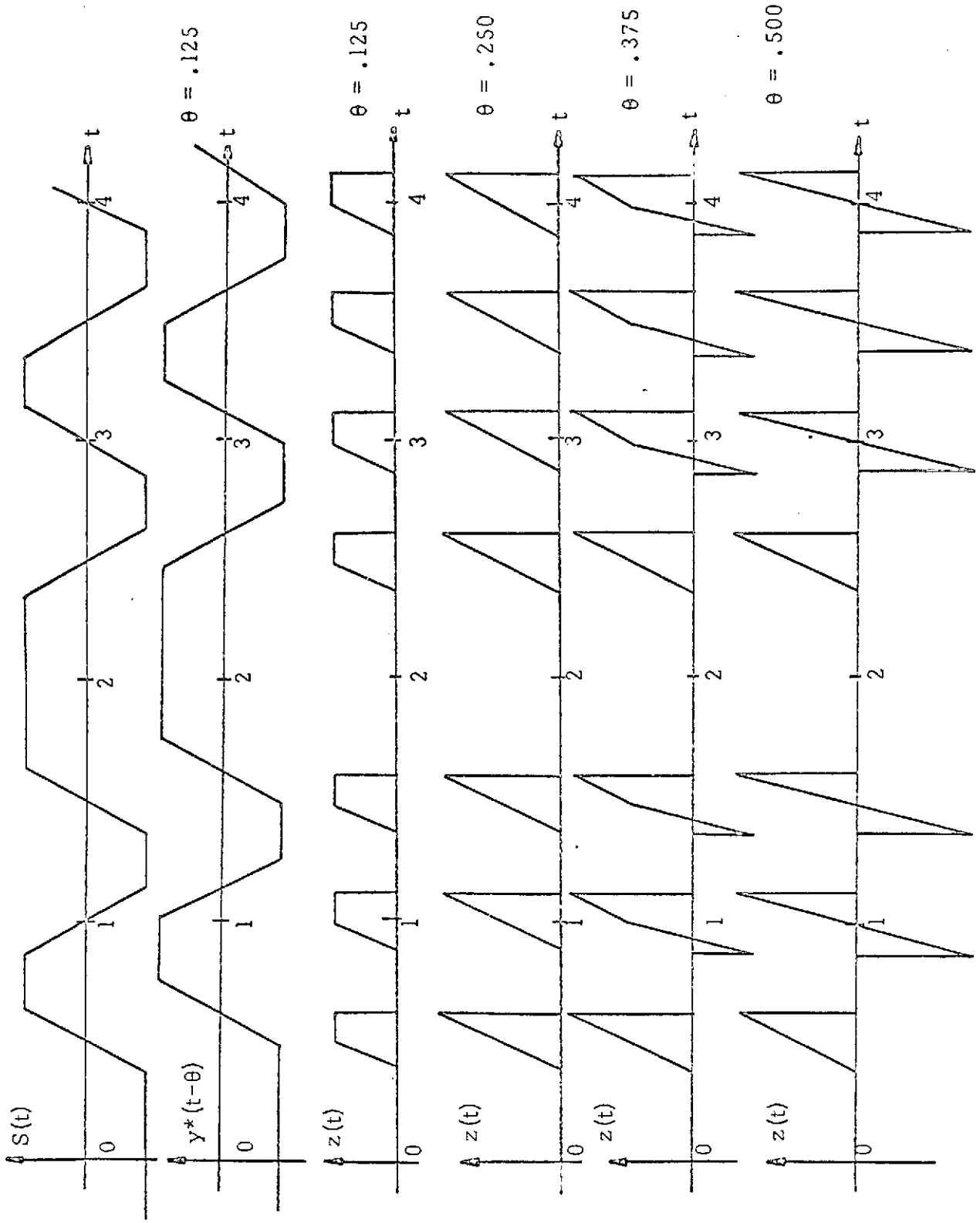


Fig. 6.11 Output waveform of the split-phase suboptimum synchronizer

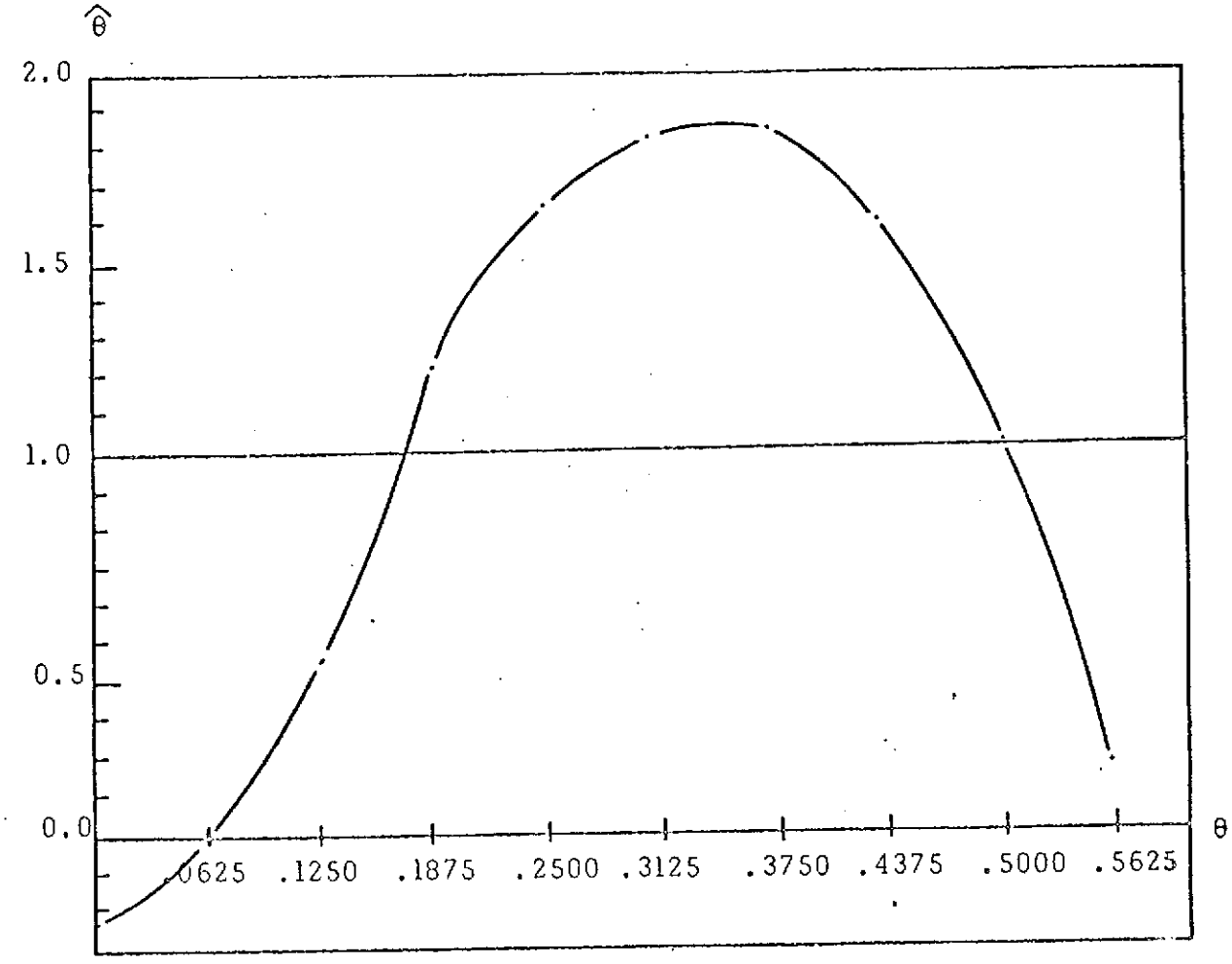


Fig. 6.12 Phase estimation from the split-phase bit synchronizer simulation program

The Fourier transform of $b_n(t)$ can be written as

$$B_n(f) = a_n \, j \, Sa(2\alpha x)[(1 - \cos x)/x] \exp(-jx(1+2n)). \quad (6.25)$$

Thus,

$$b_n(t) = \int_{-B}^{B} B_n(f) \exp(j2\pi ft) \, df$$

$$= a_n \frac{j}{\pi} \int_{-\pi B}^{\pi B} Sa(2\alpha x)[(1 - \cos x)/x] \exp(-jx(1+2n-2t) \, dx$$

$$= a_n (2/\pi) \int_{0}^{\pi B} Sa(2\alpha x)[(1 - \cos x)/x] \sin\overline{(1+2n-2t)x} \, dx$$

The signal portion is found as follows,

$$y_s^*(t) = (2/\pi) \int_{0}^{\pi B} Sa(2\alpha x)[(1 - \cos x)/x] \sin\overline{(1-2t)x} \, dx \quad (6.27)$$

## IV. TRACKING LOOP ANALYSIS

### A. Optimal Linear Estimation

In work previously reported [2], the form of an optimum synchronizer employing a Kalman tracking filter was presented. In this model the bit detector forms an estimate of the timing error based on a comparison operation involving one split-phase data bit. This output, derived from the bit detector threshold logic, is used as in input to the tracking rate portion of the conditioner. The timing estimator

is relatively slow, and works on an average of the threshold logic outputs over a period which is long with respect to the bit rate, but short with respect to tracking rate phenomena. When the central limit theorem is invoked, these averages can be considered as continuous signals with a Gaussian amplitude distribution.

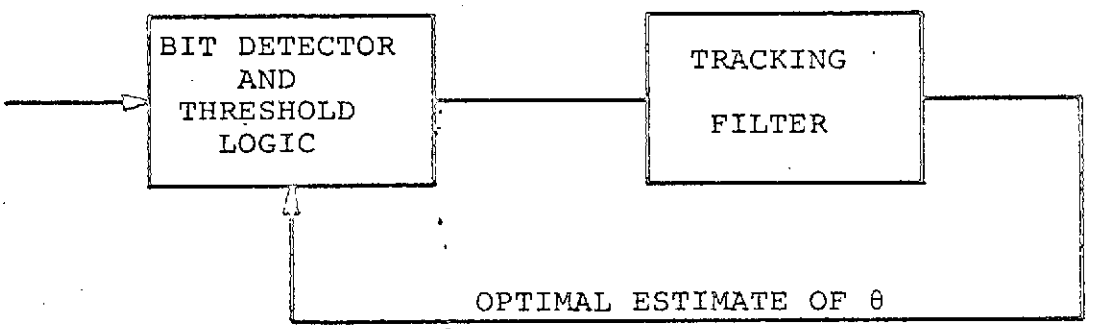


The observed signal-plus-noise vector is thus transformed, through the MAP estimator output, into a new domain such that a state vector X is linearly related to the output. That is, the MAP estimator output can be expressed in the form

$$Z(t) = H(t)X(t) + V(t),$$

where V(t) is zero mean, white, and Gaussian "measurement noise". With this interpretation of the threshold logic outputs a minimum variance estimate of the true bit transition may be obtained using the powerful Kalman filtering algorithm and making full use of known process dynamics.

1. Time Base Error

One of the more important factors which is required for this analysis is an analysis of the time-base error in the incoming recorded signal. The primary causes of this error seem to be satellite tape recorder flutter, the doppler effect, and propagation delays in the atmosphere. The most difficult cause to cope with is probably on-board tape recorder flutter, and it is necessary to model this flutter in order to optimize the tracking rate portion of the synchronizer.

Chao [12] and Moore [13] discussed measurement and causes of time-base error. Both authors give power spectra for typical instrumentation recorders. Time-base error seems to appear in two forms: a random variety, due primarily to tape disturbances, and a periodic variety, due to worn or imperfectly manufactured parts. In addition, the speed control servo, and in particular, some of its specific measurement methods, enters into the design of the tracking loop.

Worn part periodic TBE poses a difficult problem in loop optimization. Adaptive loops are generally distinctly better than fixed-parameter loops in compensating for periodic time-base error. High signal-to-noise ratio data is of particular benefit in measuring actual recorder performance, and the most effective technique is probably to use a wideband tracking loop and record the

loop output. Periodic components can then be detected by frequency analysis of this output. The Kalman filter for the tracking loop can be obtained once the power spectral density of the time-base error is known. This filter is valid for any situation where a state variable model is available and where the bit synch detector is known to be linear. This includes some, but not all acquisition problems.

As an example, a state variable model will be constructed for the flutter spectrum in Figure 9 of Chao [12]. The method of modeling a worn part will be illustrated by modeling the peak at 4 hz (which is the worst of the TBE components shown if left uncompensated) as a pair of damped sinusoidal states. The TBE will be modeled as two separate components, one resulting from the 4 hz lobe, the other from the remainder of the spectrum. The lobe (worn part) has the spectral density

$$\frac{-(.0004\%)s^2}{(\frac{4s^2}{25} + s + 100)(\frac{4s^2}{25} - s + 100)},$$

and the rest of the spectrum has the psd

$$\frac{-1}{s^2} \frac{(.01\%)^2 s^4}{(s^2 + 120s + 3600)(s^2 - 120s + 3600)}.$$

Each function can be modeled by a white noise driving a filter with a transfer function which is the spectral

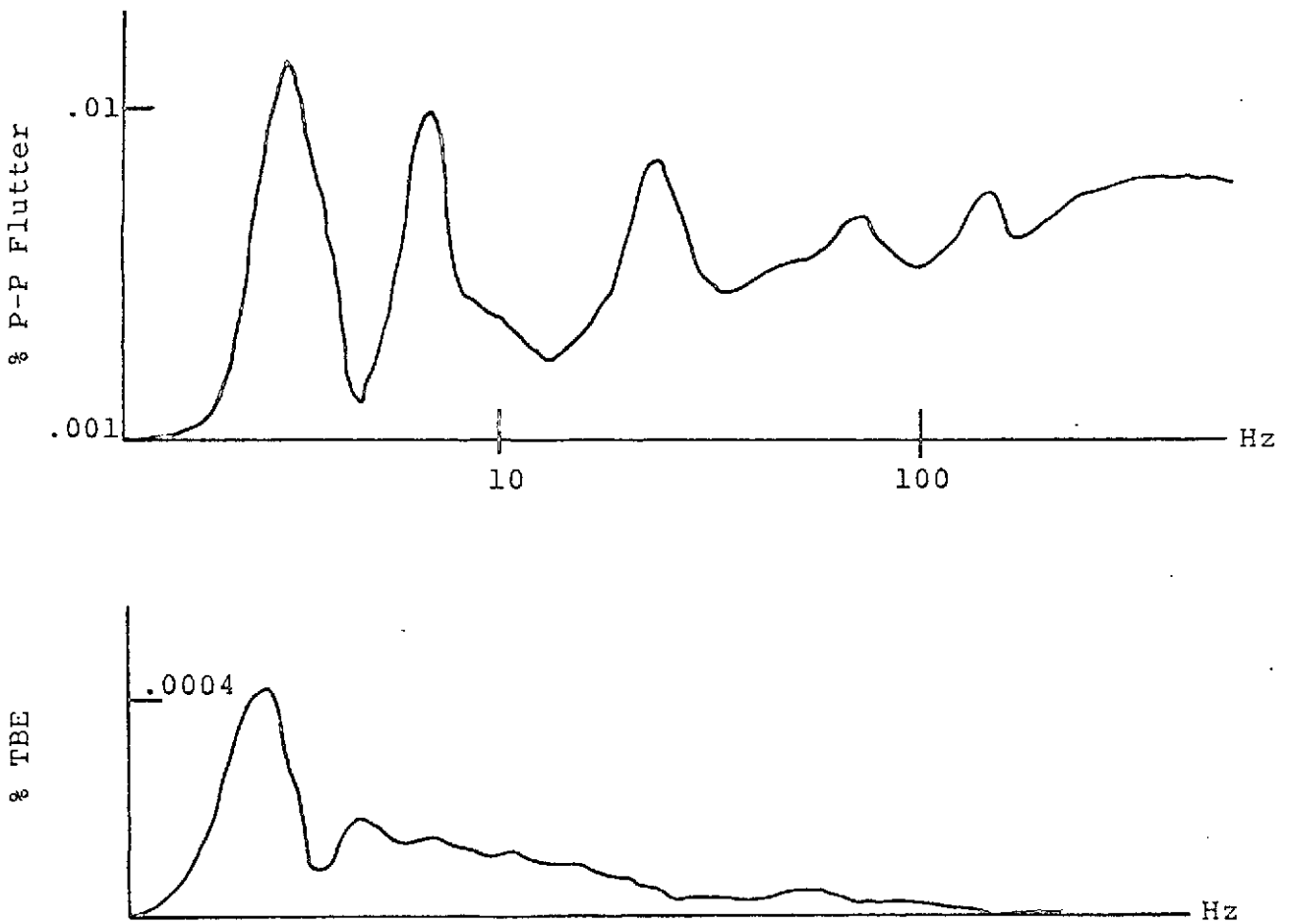


Fig. 7.1 Chao's Flutter Spectrum

factorization of the psd. A Kalman filter is then con-

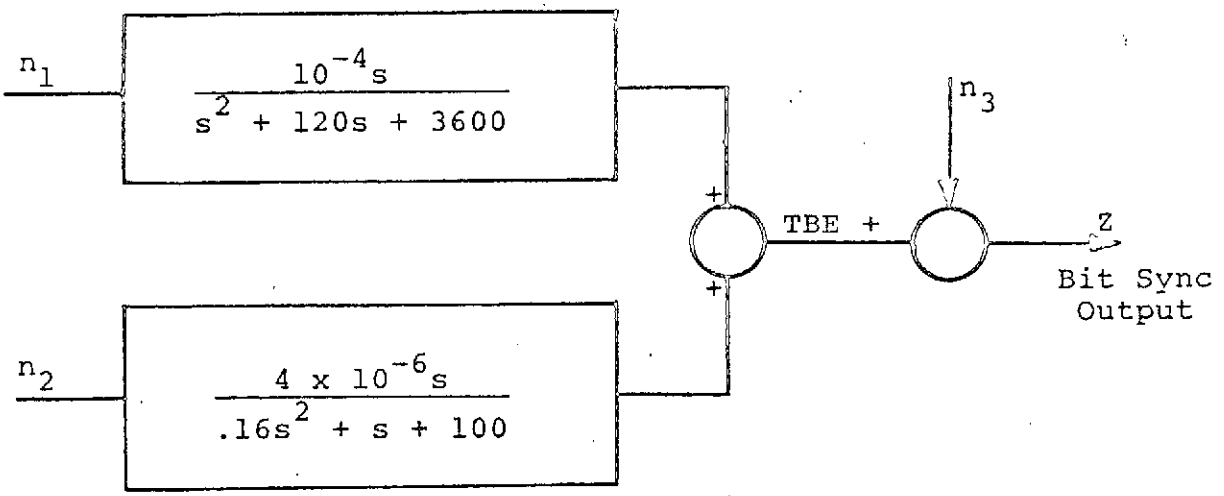


structed for this TBE model. If the worn part does or does not exist with probability 0.5, a measure of the effectiveness of an adaptive scheme would be obtained by comparing the RMS TBE with no worn part for filters designed with and without the worn part. More refined loops must be defined with more complete data than that shown.

2. Acquisition

Acquisition presents several distinct problems in the tracking loop. Stiffler (1, p138ff) develops an approximation for acquisition time for a loop with a sinusoidal nonlinearity and an initial frequency offset. The derivation is very useful in characterizing acquisition behavior of bit synchronizers. The relationship states that for a second-order loop, the acquisition time is

proportional to the square of the frequency offset and the mean square of the nonlinearity. For sinusoidal nonlinearities the mean square is one half, while for typical early-late gates it is one forty-eighth. This indicates that the bit detector, as well as the loop bandwidth may need to be changed during the acquisition phase.

It may be seen from the above discussion that the initial frequency offset is critical to the acquisition time. This offset is almost entirely a function of the speed control method used in the recorder. Specifically, if this initial frequency is accurately known, acquisition is very much simplified. Peavey [14] quotes acquisition times of one to three thousand bits for low signal-to-noise ratios. For these acquisition times, the initial frequency offset also can be contributed by the low-frequency (less than ten hertz) TBE.

Acquisition of a signal of unknown frequency and phase can be viewed as a two-dimensional search process. The synchronizer effectively looks for the element in the search area which appears to contain the signal. Acquisition can be said to occur when the probability that the signal is in a certain element of search area and no other approaches one. There is a tradeoff between equipment multiplicity, search area, and signal-to-noise ratio.

It appears possible to hypothesize a situation where acquisition might not be possible with any synchronizer,

even though tracking might be possible after acquisition has occurred. The fundamental quantity for acquisition is

$$p(y|\bar{x}),$$

where $\bar{x}$ is the tracking state vector. If $\bar{x} = (\theta, f)$ where $\theta$ and f are the phase and bit rate, respectively we have the common situation in acquisition. For acquisition to be possible $p(y|\bar{x})$ has to approach one for the correct element of volume in the search space.

Under conditions where the bit rate is well known, it is possible to perform bit synchronization at signal-to-noise ratios well below threshold by using a correlation with the frame sync pattern. For the commonly used 27 bit pattern, a useful phase data point can be obtained at noise levels twenty-seven times the usual clean sync level. The tracking loop is optimized as a sampled-data filter. The method is not likely to be successful if major TBE components exist at frequencies higher than the frame rate, and it is relatively useless for data extraction unless the noise levels fluctuate greatly.

B. Non-linear Estimation Methods

The general nonlinear filtering problem formulated for the time continuous case by Kushner and formulated for the time discrete case by Stratonovich applies to various

types of communication problems. In this chapter, the nonlinear filtering technique is used to solve the bit synchronization and detection problems when dealing with overlapping signals. The message and observation models in this study are described by the following pair of stochastic differential equations.

$$d\underline{x} = \underline{f}(\underline{x})\ dt + d\underline{w} \tag{7.1}$$

$$d\underline{y} = \underline{h}(\underline{x})\ dt + d\underline{v} \tag{7.2}$$

where $\underline{x}$ represents the state and $d\underline{y}$ is the observation. $\underline{w}$ and $\underline{v}$ are independent Wiener processes.

The general nonlinear filtering problem is the determination of $P\{\underline{x}(t) | d\underline{y}(t),\ 0 \leq t \leq T\}$, which is the probability density function of $\underline{x}(t)$ conditioned upon the observations $d\underline{y}$ on the interval $(0,T)$.

Similar results are available for the case where the observation is called $\underline{y}$ and the model is

$$\underline{y} = \underline{h}(\underline{x}) + \underline{n}(t) \tag{7.3}$$

where $\underline{n}(t)$ represents the white noise. Thus the equivalent problem for the observation equation (7.3) is the determination of $P\{x(t) | y(t),\ 0 \leq t \leq T\}$. This approach is used by Stratonovich.

The time continuous case is analyzed by solving the following filtering equation for the conditional probability density function P:

$$dP = L^{+}\{P\}\,dt + P\{d\underline{y} - E\underline{h}(\underline{x})\,dt\}^{T} V_{v}^{-1}\{\underline{h}(\underline{x}) - E\underline{h}(\underline{x})\} \quad (7.4)$$

where $P = P\{\underline{x}(t) \,|\, d\underline{y}(t),\ 0 \le t \le T\}$,

$$E\,h(x) = \int_{-\infty}^{\infty}\cdots\int \underline{h}(\underline{x})\ P\{\underline{x}(t) \,|\, d\underline{y},\ 0 \le t \le T\}\ d\underline{x}(t) \quad (7.5)$$

and $L^{+}$, Kolmogorov's diffusion operator, is defined as

$$L^{+}\{\cdot\} = -\sum_{i=1}^{m} \frac{\delta}{\delta x_i} f_i\{\cdot\} + (1/2) \sum_{i=1}^{m}\sum_{j=1}^{m} \frac{^{2}\{\cdot\}}{x_i\ x_j} \quad (7.6)$$

The filter equation for the discrete case is similar and can be found from the results of Stratonovich,

$$dP_i = \sum_{j=1}^{m} a_{ij}P_j\,dt + P_i\{dy - E\,h(x)\,dt\}V_{v}^{-1}\{h(s_i) - E\,h(x)\} \quad (7.7)$$

where $P_i = P\{x(t) = s_i(t) \,|\, dy(t),\ 0 \le t \le T\}$, (7.8)

$$E\,h(x) = \sum_{i=1}^{m} h(s_i(t)) \cdot P_i \quad (7.9)$$

and the corresponding $L^{+}$ can be described by a matrix whose elements are the transition probabilities:

$$a_{ij} = \lim_{\Delta t \to 0} \Pr\{x(t+\Delta t)=s_j(t+\Delta t) \,|\, x(t)=s_i(t)\}/\Delta t \quad (7.10)$$

$$a_{ii} = -\lim_{\Delta t \to 0} 1 - \Pr\{x(t+\Delta t)-s_i(t+\Delta t)\ x(t)=s_i(t)\}/\Delta t \quad (7.11)$$

1. An Example

Suppose we have received a sequence of binary NRZ signals with synchronization error $\theta$ and noisy observations. Find the filtering equation for the probability density function and the nonlinear bit synchronizer structure.

For the noiseless case, the observed symbol in the interval

$$[(n-1) + \theta, n+\theta], \quad n=1,2,\ldots,N$$

is

$$s^n(t) = a_n \tag{7.11}$$

A typical received signal waveform is indicated in Figure 7.1(a). To formulate the filtering equation, let us first define the following,

$$s^n_{ij} = \begin{cases} i, & \text{for } n < t \leq n + \theta \\ & \\ j, & \text{for } n + \theta < t \leq n + 1 \end{cases} \qquad i,j = -1,1. \tag{7.12}$$

and the probabilities,

$$P^n_{ij}(t,\theta)$$

$$= \Pr\{s^n(t)=i, \text{ for } (n-1) \leq t \leq (n-1+\theta);$$

$$s^n(t)=j, \text{ for } (n-1+\theta) \leq t \leq n\}. \tag{7.13}$$

where $i,j = -1,1 \qquad n=1,2,\ldots,N.$

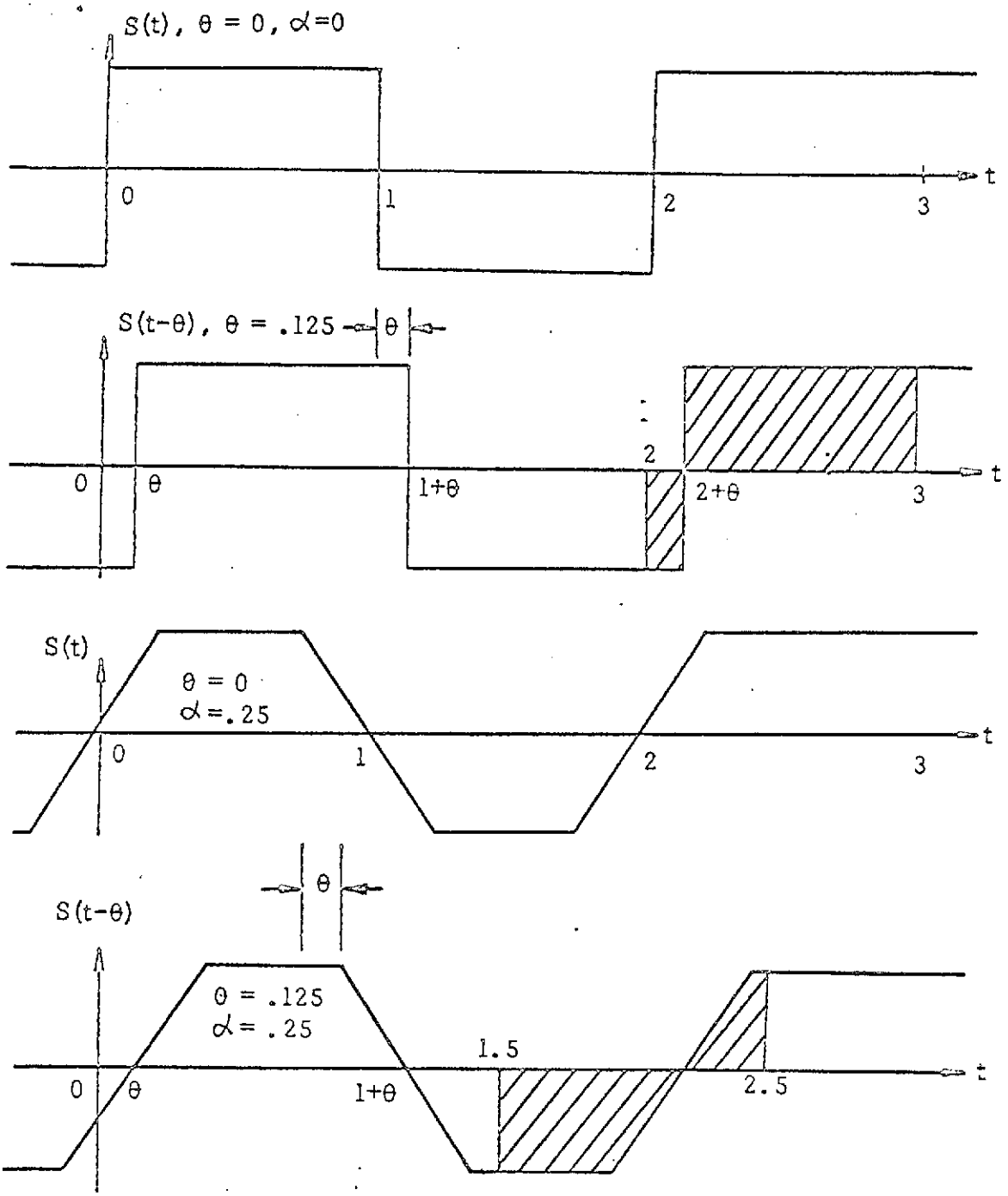


Fig. 7.1a NRZ Signal

b Overlapping Signal

Let $$\dot{y} = s^n(t) + dv/dt \tag{7.14}$$

be the observation on the interval $(n-1,n)$ and $E(dv^2) = B_o dt$ where $B_o$ is the equivalent spectral density of a white noise.

Using the result of Kushner [15], the probability $P^n_{ij}(t,\theta)$ must satisfy the following filtering equation:

$$\dot{P}^n_{ij}(t,\theta) = L^+\{P^n_{ij}(t,\theta)\} + P^n_{ij}(t,\theta)(\dot{y} - m_\theta(t))(s^n_{ij} - m_\theta(t))/B_o \tag{7.15}$$

where

$$L^+ P^n_{ij}(t,\theta) = -\sum_{i=1}^{n} \frac{\delta}{\delta x_i} f_i(x)\, P^n_{ij}(t,\theta) + (1/2) \sum_{i=1}^{n}\sum_{j=1}^{n} \frac{\delta^2}{\delta x_i \delta x_j} P^n_{ij}(t,\theta) \tag{7.16}$$

and $$m_\theta(t) = \sum_{i=-1}^{1}\sum_{j=-1}^{1} \int_{-\infty}^{\infty} s^n_{ij}(t,\theta)\, P^n_{ij}(t,\theta)\, dt \tag{7.17}$$

If $\theta$ is assumed to be constant at least for several bit periods, the term $L^+ P^n_{ij}(t,\theta)$ is zero and the equation reduces to

$$\dot{P}^n_{ij}(t,\theta) = P^n_{ij}(t,\theta)(y - m_\theta(t))(s^n_{ij} - m_\theta(t))/B_o \tag{7.18}$$

If the symbols are independent and equally probable, the following relations can be found.

$$P^{n}_{1,-1}(n,\theta) = P^{n}_{1,1}(n,\theta) = (1/2)\ P^{n-1}_{-1,1}(n,\theta) + (1/2)\ P^{n-1}_{1,1} \tag{7.19}$$

$$P^{n}_{-1,1}(n,\theta) = P^{n}_{-1,-1}(n,\theta) = (1/2)\ P^{n-1}_{1,-1}(n,\theta) + (1/2)\ P^{n-1}_{-1,-1}(n,\theta) \tag{7.20}$$

$$P^{n}_{ij}(n+1) = \sum_{\theta} P^{n}_{ij}(n+1,\theta) \tag{7.21}$$

where the summation is over all possible values of $\theta$.

Although both bits $a_n$ and $a_{n+1}$ could be estimated in each interval, it is clear that only part of the second bit has been observed and thus a better estimation can be made in the next interval. Hence the optimum estimate of the first bit in the interval $n < t < n+1$ is determined by checking whether or not the following inequality holds.

$$P^{n}_{1,-1}(n+1) + P^{n}_{1,1}(n+1) < P^{n}_{-1,1}(n+1) + P^{n}_{-1,-1}(n+1) \tag{7.22}$$

We decide $a_n = 1$ was sent if the above inequality does hold; if not, we decide $a_n = -1$. The nonlinear bit synchronizer is shown in Figure 7.2. It is obtained by solving the filtering equation, (7.18), and by using the relation described by (7.22). Thus it represents a combined synchronizing and estimation scheme which is optimum in the sense that it makes bit by bit decisions conditioned upon all observations up to that time. This technique can be

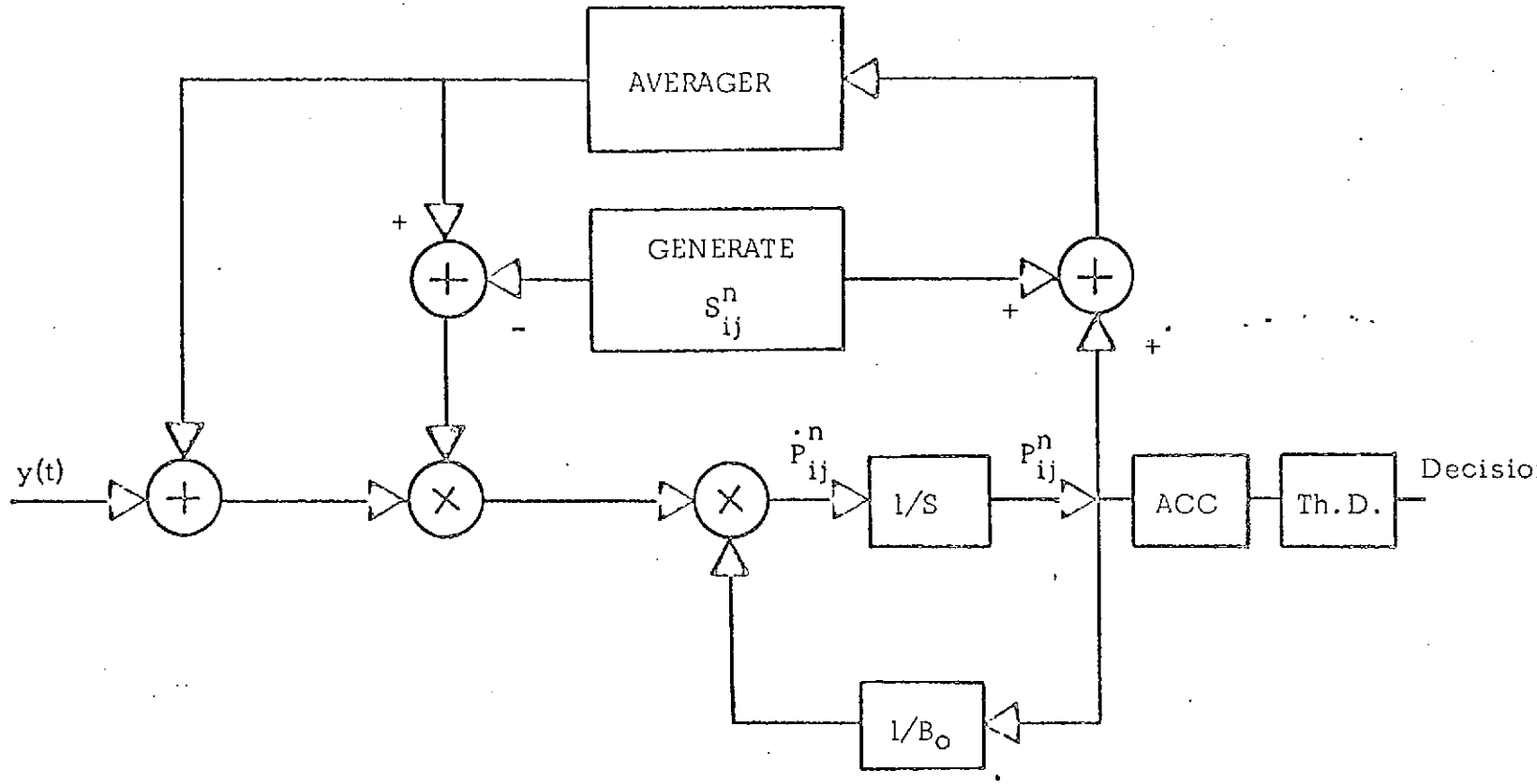


Fig. 7.2 Nonlinear bit synchronizer for NRZ signals

implemented with analog computers since the only nonlinear elements required are multipliers.

C. Nonlinear Bit Synchronizer for Overlapping Signals

For the overlapping signal case as shown in Figure 7.1(b), the message and observation models are modified in order to set up a filtering equation. Let the observed symbol in the interval

$$[(n-1) - \alpha + \theta,\ n + \alpha + \theta],\ n=1,2,\ldots,N$$

be

$$s^n(t) = a_n S_p(t). \tag{7.23}$$

where $S_p(t)$ is the overlapping symbol defined in Chapter III.

Using the same approach as Eq. (5.6), we again consider the following set of intervals,

$$[n - (1/2),\ n + (1/2)],\ n=1,2,\ldots,N.$$

and define the following functions:

$$S_{ij}^n(t,\theta) = \begin{cases} a_n S_p(t-\theta-n) & \text{for } (n - .5) \leq t \leq (n+\theta+\alpha) \\ a_{n+1} S_p(t-1-\theta-n) & \text{for } (n+\theta-\alpha) < t \leq (n + .5) \end{cases} \tag{7.24}$$

where $i \leftrightarrow a_n$, $j \leftrightarrow a_{n+1}$, $n=1,2,\ldots,N$.

The related waveform for $a_n = 1$ and $a_{n+1} = -1$ is indicated by Figure 7.3 in the interval $(n - 1/2)$, $(n + 1/2)$. We also

need to define the following probabilities:

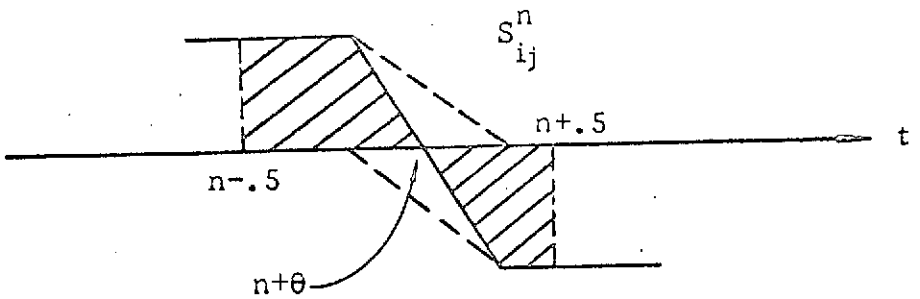


Fig. 7.3. $S_{ij}^n$ and the signal waveform in the interval (n - .5, n + .5)

$$P_{ij}(t,\theta) = \Pr\left[\begin{array}{l} s^n(t)=a_n S_p(t-\theta-n), \quad \text{for } (n-.5) \le t \le (n+\theta+\alpha); \\ \\ a^n(t)=a_{n+1} S_p(t-\theta-n-1), \quad \text{for } (n+\theta-\alpha) < t \le (n+.5) \end{array}\right] \tag{7.25}$$

where $a_n \leftrightarrow i$, $a_{n+1} \leftrightarrow j$, $i,j = 1,-1$.

Then the observation model on the interval (n - .5, n + .5) can be written as follows

$$\dot{y}(t) = S_{ij}^n(t,\theta) + dv/dt, \tag{7.26}$$

where $E(dv^2) = B_o dt$.

Substituting (7.24) into (7.26), we have

$$\dot{y}(t) = \{a_n S_p(t-\theta-n) + a_{n+1} S_p(t-\theta-n-1)\} + dv/dt$$

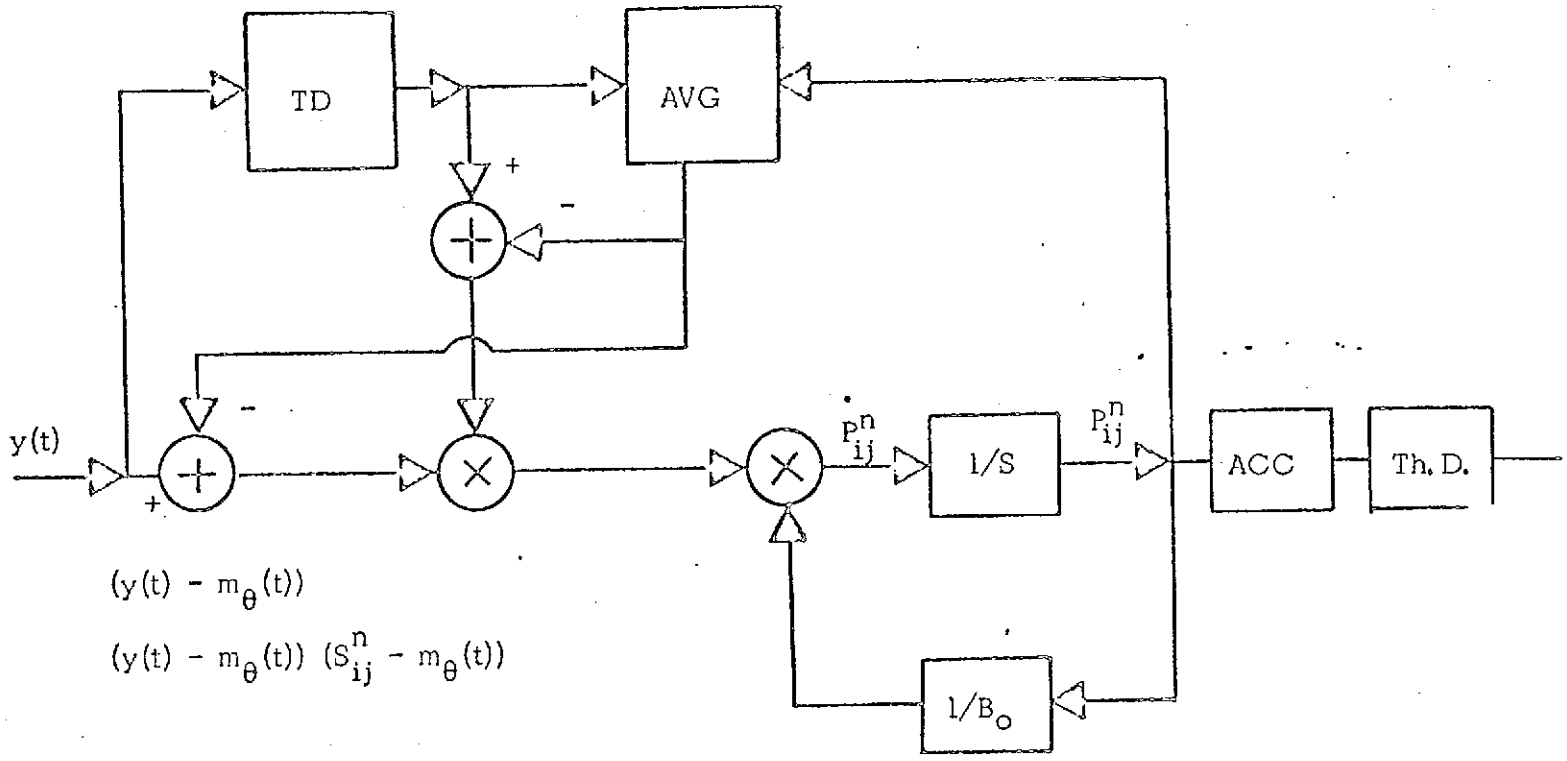


Fig. 7.4 Non'linear bit synchronizer for overlapping signals

The filtering equation can be found as follows.

$$\dot{P}^n_{ij}(t,\theta) = L^+ P^n_{ij}(t,\theta) + P^n_{ij}(t,\theta)(y - m_\theta(t))(S^n_{ij}(t,\theta) - m_\theta(t))/B_o \qquad (7.27)$$

where

$$m_\theta(t) = \sum_{i=-1}^{1} \sum_{i=-1}^{1} \int_{-\infty}^{\infty} S^n_{ij}(t,\theta)\ P^n_{ij}(t,\theta)\ dt \qquad (7.2\,)$$

The bit synchronizer structure by solving (7.27) is shown in Figure 7.4. The received signal is passed through a transition detector to form the function $S^n_{ij}(t,\theta)$. The rest of the structure is similar to the synchronizer developed in Section B of this chapter.

## V. MISCELLANEOUS TOPICS

### A. False Lock Detection

The split-phase waveform used in many telemetry systems has the advantage that it has zero average value, independent of data bit sequence, and very little low frequency content. Also, the split-phase waveform has a transition in the middle of every bit, which fact can be used to assist in detection and synchronization.

With many types of synchronizers, however, it is possible to be in sync one-half bit out of phase on split-phase signals. In order to detect or synchronize split-phase data, it is usual to invert the sign of the integrator

at mid-bit to obtain the full plus one or minus one energy. A matched filter for false lock can be constructed by using an integrate and dump over the full bit. Since missed transitions occur with probability $\frac{1}{2}$ for equiprobable and independent adjacent bits, the false-lock condition quickly becomes evident by the existence of missed transitions: The output is zero if there is a transition and plus or minus one if integrated over a missing transition.

If $y_i$ is the output of the missed transition detector for each bit, the likelihood ratio

$$\frac{p(y|H_1)}{p(y|H_0)} = \Pi\left[p_1 + (1-p_1)\exp\frac{-T}{N_o}\cosh\frac{2Ty_i}{N_o}\right]$$

where $p_1$ is the probability of an end-of bit transition. For real data it is at least one half, since such data can contain many zeros. The actual detector is implemented by using a threshold on the posteriori probability of $H_1$.

$$\frac{p(H_1|y)}{p(H_0|y)} = \frac{p(y|H_1)\ p(H_1)}{p(y|H_0)\ p(H_0)}$$

$$\text{or} \qquad \ln\frac{p(H_1|y)}{p(H_0|y)} = \ln\frac{p(y|H_1)}{p(y|H_0)} + \ln\frac{p(H_1)}{1-p(H_1)}$$

The complete false lock detector is implemented by computing

$$\Lambda = \sum\log\left[p_1 + (1-p_1)\exp\frac{-T}{N_o}\cosh\frac{2Ty_i^{\,2}}{N_o}\right]$$

$$+ \log p(H_1)$$

This statistic is quite sensitive to $p_1$. However, if a conservative value of $p_1$ is used the detector can be successfully used. The configuration is

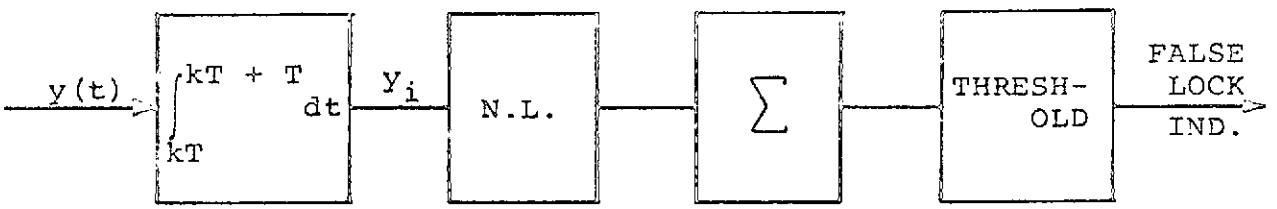


The detector is ordinarily used with an up-down counter and limiter. This provides for a reasonably quick decision, but it may not detect false lock with data with $p_1$ appreciably greater than 1/2.

B. Bit Synchronizer Evaluation Techniques

It has been suggested that some useful and easily applied performance measure, or alternatively, a simple performance test, be applied to bit synchronizer-detectors. Peavey [14] has given results of testing on actual synchronizers with typical time-base error patterns. The performance was marked by mixed behavior with respect to various criteria. For example, one would perform better at low signal-to-noise rations, another at high, one would show better cycle slipping performance, one would be more resistant to worn part TBE, and so on. Under such conditions, testing becomes a very time consuming task, and specification and selection a most emotional matter. The problem can be narrowed down considerably by considering the following inputs to the selection of a metric:

1. The mix of available data
2. Optimum synchronizer performance
3. Data recovery capability

The significant data characteristics for the satellite telemetry applications of this study are:

1. Data rate
2. Additive noise PSD
3. Pulse shape before IF filtering
4. IF filter characteristic
5. Frame length
6. Tape recorder TBE spectrum
7. Receiver carrier tracking loop bandwidth and cycle slipping probability

The first four characteristics relate to bit-rate phenomena and the last three to tracking rate.

Synchronizer performance may be characterized by the following measures:

1. Probability of bit error with additive noise and typical recorder time-base error

2. Cycle slipping probability with additive noise and typical recorder time-base error

3. Acquisition time with additive noise and typical recorder time-base error

4. Probability of bad data acknowledgement under various circumstances

In general, additive noise varies over quite a wide range in typical satellite applications. In contrast, recorder performance is not affected by orbital parameters, and thus once a suitable recorder model is obtained, it or two or three subclasses or recorder model, to account for various states of repair, are sufficient. The measures of synchronizer performance stated above are then primarily

curves of performance criteria versus signal-to-noise ratio with recorder model as a parameter. This suggests a performance index based on two or three recorder models.

Measures of data recovery capability are determined to a considerable extent by operational considerations. The range of signal-to-noise ratios encountered can usually be predicted from knowledge of the orbital parameters and the communication system data. In addition, user criteria are of interest. For example, many users do not care about occasional bad points, but they do require a knowledge of which data are invalid. Cycle slips in general cause a loss of either one or two frames of data, and thus a cycle slip should be weighted as heavily as a frame of bit errors. As a result, the following measure of bit synchronizer merit is tentatively suggested:

$$M = \int_{R_{min}}^{R_{max}} \frac{p(E|R) + F\, p(\text{cycle slip}|R)}{p_{opt}(E|R)} W(R)\, dR,$$

Where $R_{min}$ and $R_{max}$ are the minimum and maximum signal-to-noise rations to be expected in useful operation, R is the signal-to-noise ratio, F is the frame length, and W(R) is the operational requirement weighting function. If wide variations of recorder performance are to be expected in practice then a weighted average of M taken at several signal-to-noise ratios should be used.

An additional important consideration is that of recorded signal bandwidth. This criterion should depend on the mix of recorded signal bandwidths to be expected in practice. The test should be based on a signal with a fairly realistic but reasonably easily generated TBE pattern. One possibility is a flat flutter spectrum passed through a representative speed control filter with a representative worn part component at a worst case frequency.

## Conclusion

The primary accomplishments of this study have been in the analysis and simulation of receivers and bit synchronizers. It has been discovered that tracking rate effects play a rather fundamental role in both receiver and synchronizer performance, but that data relating to recorder time-base-error (TBE), for the proper characterization of this phenomenon, is in rather short supply.

It is possible to obtain operationally useful tape-recorder TBE data from high signal-to-noise ratio (SNR) tapes using synchronizers with relatively wide-band tracking loops. Low SNR tapes examined in the same way would not be synchronizable. One of the aims of any future study in this area should be the development of effective methods for testing and evaluating existing synchronizers. For this type of testing a realistic TBE model is a necessity. Experimental data, taken from existing tapes for which statistical data such as that recorded at GSFC tape quality or tape evaluation laboratories is available, should be examined in an effort to correctly define satellite on-board tape recorder data characteristics. The techniques developed in this report can then be applied to the optimization of bit synchronizer models. It is possible

that considerable improvement can be made in synchronizer performance with such models.

Additional topics of interest are receiver false lock, cycle slipping, and other unusual phenomena, which have been described to some extent in this and earlier reports and simulated during the study.

## References


1. Stiffler, J. J., Theory of Synchronous Communications, Prentice-Hall, Inc., Englewood Cliffs, N. J., 1971.

2. Noack, T. L., and Morris, J. F., "Digital Data Detection Study", Progress Report June 1, 1969 - November 1, 1969, NASA Grant NGR26-003-044, Goddard Space Flight Center, Washington, D. C.

3. Van Trees, H. L., Detection, Estimation and Modulation Theory, Part I, John Wiley & Sons, New York, N. Y., 1968.

4. Aaron, M. R., and Tufts, D. J., "Intersymbol Interference and Error Probability", IEEE Trans. on Information Theory, Vol. IT-12, January, 1966.

5. Helstom, C. W., Statistical Theory of Signal Detection, Pergamon Press, New York, N. Y., 1960.

6. Thumin, A. I., "PCM Bit Detection with Correction for Intersymbol Interference", Tech. Memo. #64, Lab. for Electroscience Research, New York Univ., Bronx, N. Y., 1966.

7. Wang, Chung-Tao David, "Performance of Self-bit Synchronizers for Binary Overlapping Signals", Ph.D. dissertation, University of Missouri-Rolla, 1972.

8. Wintz, P. A., and Luecke, E. J., "Performance of Optimum and Sub-optimum Synchronizers", IEEE Trans. on Communication Technology, Vol. COM-17, June, 1969.

9. Simon, M. K., "Non-linear Analysis of an Absolute Value Type of Early-Late-Gate Bit Synchronizer", Proc. Nat'l Telemetry Conf., Washington, D. C., 1969.

10. Stiffler, J. J., "On the Performance of a Class of PCM Bit Synchronizers", Proc. National Telemetry Conf., Washington, D. C., 1969.

11. Wang, C. David, Noack, T. L., and Morris, J. F., "Maximum Likelihood Synchronizer for Binary Overlapping Symbols", Proc. Region III IEEE Conference, May, 1973.

12. Chao, S. C., "Flutter and Time Errors in Magnetic Data Recorders", Int. Telemetry Conf., Los Angeles, Calif., 1965.

13. Moore, Laurence, "The Effects, Measurement, and Analysis of Flutter in Instrumentation Recorders", Proc. Int. Telemetry Conference, Los Angeles, California, 1968.

14. Peavey, B., "Performance Characteristics and Specification of Bit Synchronizer/Signal Conditions", Proc. International Telemetry Conf., Los Angeles, Calif., 1968.

15. Kushner, H. J., "On the Differential Equations Satisfied by Conditional Probabilities of Markov Processes with Applications", SIAM Journal on Control, No. 2, 1964.

16. Stratonovich, R. L., Conditional Markov Processes and Their Application to the Theory of Optimum Control, American Elsevier, 1968.